M.6 References

M1. "**Icing Design Envelopes (14 CFR-25, 29, Appendix C) Converted to a Distance-Based Format,**" Richard K. Jeck, FAA Technical Report DOT/FAA/AR-00/30 (2000), FAA Technical Center, Atlantic City, NJ 08405.

M2. "**A New Database of Supercooled Cloud Variables for Altitudes up to 10,000 Feet AGL and the Implications for Low Altitude Aircraft Icing,**" Richard K. Jeck, DOT/FAA/CT-83/21 (1983), FAA Technical Center, Atlantic City, NJ 08405.

M3. Aviation Weather Center: http://www.awc-kc.noaa.gov

M4. National Weather Service: http://weather.noaa.gov

M5. **An Inferred Climatology of In-Flight Icing and SLD for North America**, Bernstein, B.C., Proceedings of the 10th American Meteorological Society Aviation Range and Aerospace Meteorology Conference, Portland, Oregon, May, 2002, pp. J21-J24.

M6. American Meteorological Society, 45 Beacon Street, Boston, MA 02108-3693. Tel: 617-227-2425. Internet: http://www.ametsoc.org.

M7. Society of Automotive Engineers: http://forums.sae.org/access/dispatch.cgi

M8. "**Designated Engineering Representatives Consultant Directory,**" Advisory Circular No. 183.29-1HH (2000), Federal Aviation Administration, 800 Independence Ave. SW, Washington, DC 20591.

APPENDIX N. WAYS TO EVALUATE ICING EXPOSURES RELATIVE TO APPENDIX C.

N.1 Background.

Measured natural icing flight test conditions should be documented. The methods contained in N.2 may be used to compare the measured natural ice test conditions to Appendix C.

Appendix C envelopes as shown in Figures D-1 and D-4 of Appendix D are valid *only* for averaging distances of 17.4 nmi and 2.6 nmi, respectively. Most of the time, icing encounters in flight will cover shorter or longer distances. In order to compare the flight data with the envelopes, the data should be averaged over the same distances for which the envelopes are drawn. This is not always possible, especially if the encounters are shorter than the design distances. It is improper to use the F-factor curves in Figures D-3 (Figure 3 of Appendix C) and D-6 of Appendix D (Figure 6 of Appendix C) to adjust the encounter-averaged LWC to equivalent values over 17.4 nmi or 2.6 nmi. The F-factor curves should be used to adjust the LWC curves in Appendix C to match each of the actual averaging distances obtained from the test flights.

The Appendix C envelopes treat LWC and MVD as principal variables with exposure distance treated as a constant. For comparison with test data, distance may be a more useful variable, and the envelopes may be redrawn for fixed values of MVD. Statistical analysis of MVD measurements in the atmosphere suggest that MVDs are much less variable than may be generally realized[1]. However, for presenting certification data, the applicant should provide MVD data for each particular encounter.

N.2 Appendix C Converted to Distance- or Time Based Envelopes.

The F-factor curves can be used to convert Figures D-1 and D-4 of Appendix D to an equivalent LWC versus Horizontal Extent (HE) format [N1]. Figure N-1 shows conversion of Appendix C envelopes shown in Figures D-1 and D-4 to a distance-based format for temperatures of 0° C, -10° C, -20° C, and -30° C and for an MVD of 15 μm. As explained in [N1], after entering the basic coordinates into a computerized spreadsheet, variations or customized versions of the envelopes can be easily generated using the spreadsheet charting capabilities. For example, in Figure N-1 a logarithmic HE scale has been chosen in order to accommodate both the short HEs of the Intermittent Maximum envelopes and the long HEs of the Continuous Maximum envelopes.

Natural icing atmospheric measurements can be plotted on Figure N-1 for MVDs near 50 μm, or on similar graphs for other MVDs near 15 μm, no matter what the horizontal extents or averaging distances**.**

[1] Statistics compiled at the FAA Technical Center from 12,000 nmi of measurements in stratiform icing conditions revealed that about 75 percent of all MVDs are within ± 5 μm of 15 μm in stratiform clouds.

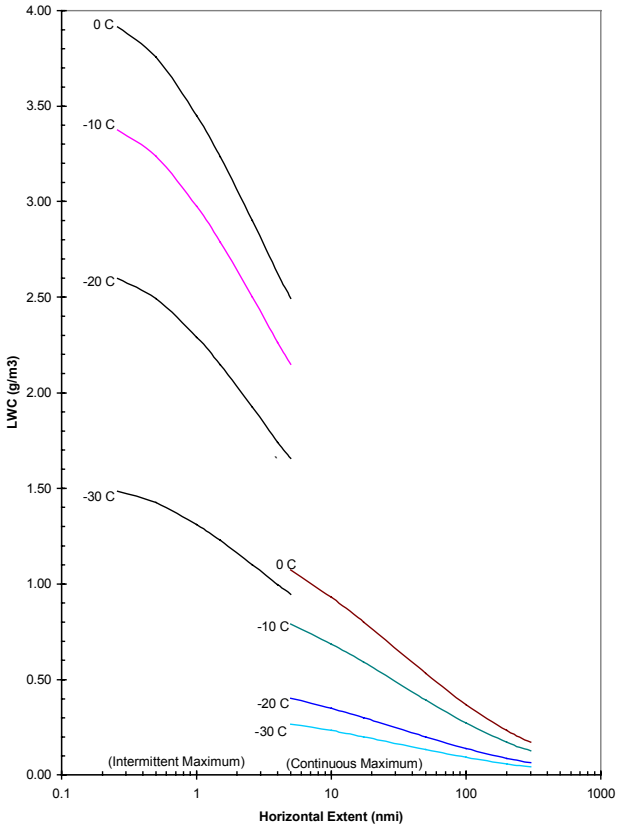

Figure N-1. 14 CFR Parts 25 and 29 Appendix C icing envelopes converted to a distance-based format (for MVD=15 μm).

Inflight exposures may be measured in terms of the distance flown in the icing condition or in terms of elapsed time. Icing wind tunnel exposures and computer simulations are typically reported as timed exposures. The distance-based format can be converted to a time-based format by dividing the distance scale by the airspeed, assuming that the flight speed is approximately constant during the cloud penetration. For example, at 200 knots, the 200 nmi mark is also the 60 minute mark. The 20 nmi mark is also the 6 minute mark, and so on.

For use of the time-based format, the time scale must be renumbered for each airspeed in use. Note that this time-based format allows wind tunnel and computer simulated exposures and flight test averages to be plotted on the same time-based 14 CFR parts 25 and 29 Appendix C envelopes, if the airspeeds are similar.

N.3 References

N1. "**Icing Design Envelopes (14 CFR-25, 29, Appendix C) Converted to a Distance-Based Format,**" Richard K. Jeck, FAA Technical Report DOT/FAA/AR-00/30 (2000), FAA Technical Center, Atlantic City, NJ 08405.

APPENDIX O. USING ICING RATE TO DOCUMENT ICING EXPOSURES

O.1 Background.

In icing flight tests there has always been a need to document the characteristics or quality of icing exposures in some meaningful way, in addition to documenting the MVD, LWC, temperature, and exposure time. In the absence of any previous guidance on this topic, various schemes have been devised by applicants or by icing data analysts. Some of these schemes are erroneous, and none of them appear to be entirely legitimate or satisfactory. In the interest of promoting a sound, useful and understandable way to document icing exposures, the following method, based on the use of an icing rate sensor, is recommended.

Applicants may use a suitable icing rate sensor as one of the onboard instruments for icing flight tests. These devices are small, relatively inexpensive, and easy to use. Related models of ice detectors may already be installed on the aircraft as standard equipment.

O.2 Data from an Icing Rate Sensor.

To illustrate the use of icing rate for documentation purposes, data from a Goodrich model 871FA icing detector will be described as an example. This model provides a voltage output signal which is normally set to increase from 1 to 5 volts as ice accretes on a ¼-inch diameter sensing rod exposed to the airstream. The output is 1 volt when the rod is ice free, and is 5 volts when about 0.5 mm of ice has accumulated on the rod. At the 5 volt level, a heater is energized for a few seconds to melt the ice off the rod, and the ice accretion can resume, starting a new cycle, when the rod cools to below 0 °C again.

A recorded trace of this output signal, as in Figure O-1, gives a clear indication of when icing occurred during the flight – three main encounters and two brief ones. A close-up view of the signal (Figure O-2) shows the detailed characteristics of the signal and shows how the icing rate is computed for each of the cycles. An average icing rate over each of the icing intervals seen in Figure O-1 would sufficiently document the icing rate for the interval.

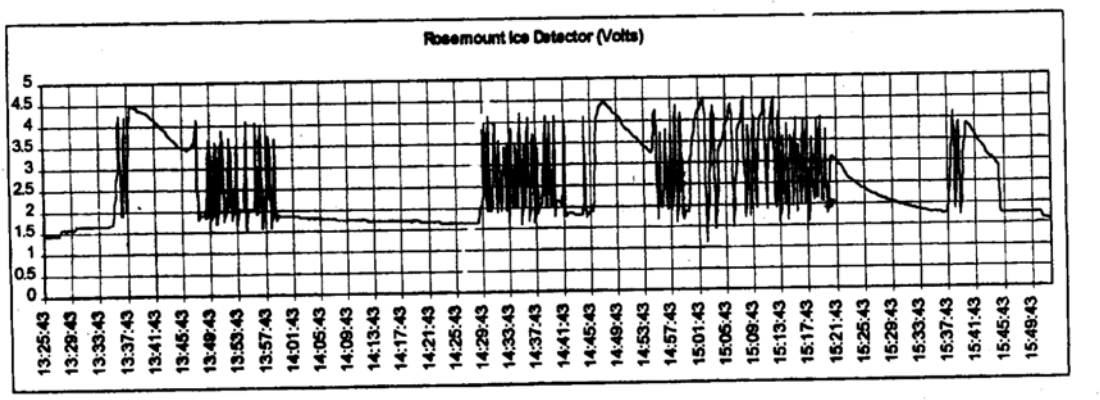

Figure O-1. Actual Example of the Analog Output Voltage from a Model 871FA Ice Detector During an Icing Encounter.

The record in figure O-1 clearly shows when icing exposures occurred. The number of up-and-down cycles per unit time gives a rough idea of the icing intensity at a glance on the time-compressed display shown here. Precise values of the icing intensity can be obtained easily from the individual cycles when recorded second-by-second, or when displayed on an expanded time scale as in the figure O-2.

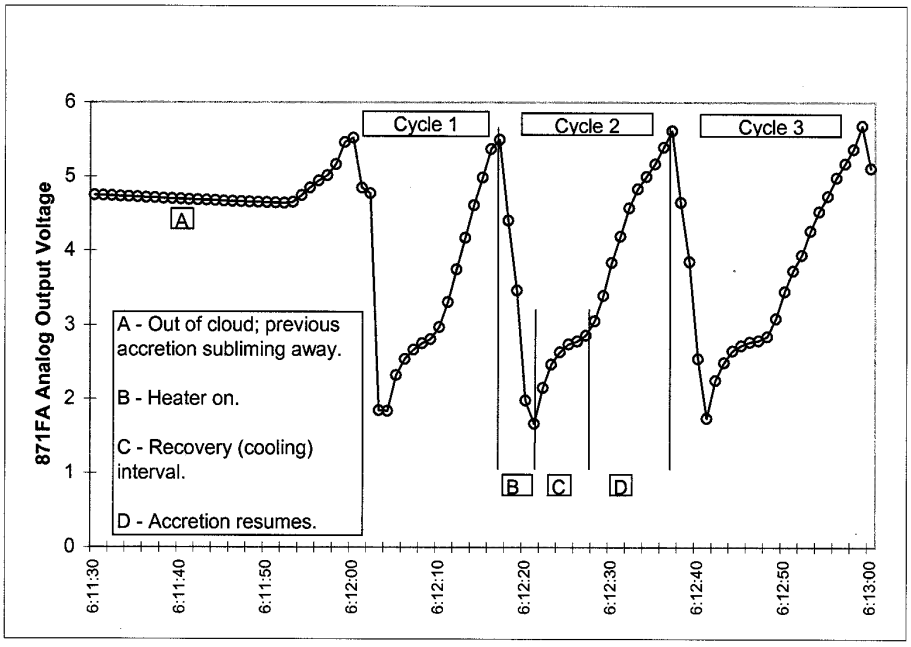

Figure O-2. High Resolution Example of Analog Output Voltage from an 871FA Ice Detector.

For model 871FA icing detectors normally set for a sensitivity of 0.5 mm of ice over a 4-volt output range (1-5 v, approximately), the ice accretion rate in mm/min is given simply by

$$\text{Rate(mm/min)} = 7.5 \times \text{dV(volts)/dt(sec)}$$

Where dV/dt is the ratio of the voltage increase over a time interval (dt) during the accretion phase of an individual cycle. This can be computed easily from the record if the output voltage is recorded every second as in figure O-2. The icing rates computed for the accretion phase of cycles 1-3 in this example are 3.1, 2.1, and 1.9 mm/min, respectively.

O.3 Converting Icing Rate to Icing Intensity.

For evaluation purposes, the icing rate (mm/min) indicated by the sensor can be conveniently related to familiar icing intensity terms, as shown in Table O-1. For example, a rate of 1 mm/min indicates a moderate icing rate on the ¼-inch sensing rod, according to this scale. These intensities apply at any airspeed – it is only the rate of accretion that matters.

Table O-1. Measurable Definitions of Icing Intensity2

Intensity	Rate (mm/min)	Equivalent Rate
Light	0.1 to 0.4	¼ to 1 inch / hour
Moderate	0.4 to 1.3	1 to 3 inches / hour
Heavy	> 1.3	> 3 inches / hour

As explained in references [O1] and [O2], these rates may be applied universally to any component of the aircraft as well. Thus, if the wing is collecting ice at the rate of 0.9 mm/min (2 inches per hour), then that is a moderate icing rate for that wing. (A different aircraft at a different airspeed may collect ice at a different rate in the same icing conditions.)

The rate measured by the icing rate sensor will be different from the rate of accumulation on the wing, due to the difference in size and therefore to the difference in droplet collection efficiencies between the two. The icing rate and intensity on the wing can nevertheless be conveniently estimated from the rate indicated by the icing rate sensor. For present purposes, this can be done simply by using the ratio of the collection efficiencies,

$$Rate_{wing} = (ß_{wing}/ß_{sensor}) x Rate_{sensor}$$

where the peak local collection efficiencies, ß, can be obtained easily from LEWICE or other ice accretion computer codes [O3]. Thus, for a ratio of $ß_{wing}/ß_{sensor} = (0.3/0.9) = .33$, the wing will collect ice at about a third of the rate on the icing detector.

O.4 Data Sheet for Documenting Icing Exposures

A suggested format for documenting icing exposures in terms of icing rates and intensities is illustrated by the example given in Table O-2. The top half of the form lists pertinent information about the test aircraft and the icing conditions in general. The lower half of the form contains details of the individual icing encounters, as follows:

- Columns A-D identify the selected icing intervals from Figure O-1.
- Column F lists the average icing rates computed as indicated in Figure O-2.
- Column G lists the equivalent icing intensities on the ¼-inch diameter sensor, using Table O-1.
- Columns I and J are the estimated rates and intensities for the aircraft component of interest – in this case the leading edge of the outer wing.
- Column K contains the cumulative product of Rate x Duration, as obtained from columns I and C.
- Columns P and Q keep track of any usage of the ice protection system during the flight.
- Columns S-W provide a way to document the performance and handling qualities of the aircraft as a result of the icing encounters. The numerical entries in these columns are based on the level-of-effects scale shown in Table O-3.
- Columns Y-AA allow for other data, such as from an LWC meter and a droplet sizing instrument or droplet impactor slide.

2 This scale has been proposed as part of a revision to the official icing intensity definitions promulgated in the Aeronautical Information Manual (AIM) . The revisions have been recommended by an interagency working group assembled in response to Task 1-B of the FAA Inflight Aircraft Icing Plan of 1997 .

Table O-2. Suggested Data Sheet for Documenting Icing Exposures

Icing Exposure Record for Flight Tests (hypothetical numbers inserted for illustrative purposes.)

Aircraft model & S/N: B-210, S/N=1416 Component(s) of interest: outer wing LE

Type of ice protection system: boots

Date of Flight Test: Nov. 12, 2007 Flight Number: 2

Location: western Kansas

General cloud type(s) and conditions: deep, widespread stratus & low ceiling:(cloud base = 1000 Ft AGL @ -2C, cloud tops = 4200 Ft AGL @ -12C)

Height of freezing level (AGL): sfc to 500 (feet)

Starting with an ice-free aircraft (and no descent into warm air for de-icing)

	Exposure			On 871FA Icing Rate Meter		On Component of Interest**			Other Conditions					-- Aircraft Performance and Handling --					Auxiliary Data		
	Start-End Time	Duration	Distance	Average Icing rate	Equivalent Intensity*	Average Icing rate	Equivalent Intensity*	Cumulative Ice Depth	Altitude	OAT	TAS	No. of IPS cycles during exposure	No. of IPS cycles after exposure	Level of Effect (1,2,3, or 4) on Aircraft*** Speed	Power	Climb	Control	Vibration	Average LWC (g/m3)	MVD (μm)	Engine Pwr or EPR
No.	(hhmm:)	(min.)	(nmi)	(mm/min)	(T,L,M,H)	(mm/min)	(T,L,M,H)	(mm)	(Ft, ASL)	deg C	(kt)										
1	1430 - 1441	11	28	0.7	M	0.35	L	3.9	7500	-11	150	2	1	1	1	untested	1	1			
2	1455 - 1459	4	10	0.4	L	0.2	L	4.7	7400	-10	"	0	1	1	1	"	1	1			
3	1502 - 1514	12	30	0.2	L	0.1	T-L	5.9	7000	-9	"	0	0	1	1	"	1	1			
4	1514 - 1521	7	18	1	M	0.5	L-M	9.4	7500	-11	"	2	1	1	2	2	1	1			
	Sums:	34	86																		

Notes:

* Icing intensity scale is that proposed by FAA Icing Plan Task-1B working group (2001). (T= <0.1 mm/min, L = 0.1 - 0.4 mm/min, M = 0.4 - 1.3 mm/min, H = >1.3 mm/min)

** These amounts are merely approximations for estimation and comparison purposes only. They are computed from the 871FA data simply by using the ratio of the collection efficiencies.. They give a rough idea of what may accumulate if no IPS is active on the component of interest.

*** Level-of-effect scale is that proposed by FAA Icing Plan Task-1B working group (2001). (See separate Table of Effects with definitions.)

Although Table O-3 is intended for use with aircraft having approved ice protection systems, it should also be used to report effects of icing encounters on any aircraft.

The example data in Table O-2 show that the outer wing of the test airplane was exposed to mostly light icing for 34 minutes (86 nmi). After the end of the combined 86 nmi exposure, only the power and climb capability showed any significant (level 2) degradation. This degradation occurred even though the boots were cycled several times during the encounter. If the boots had not been used, an estimated 9.4 mm (3/8-inch) of ice would have accumulated on the outer wing.

The data sheet in Table O-2 is an acceptable way to document icing exposures. If an icing rate sensor is not available, applicants are encouraged to use the data sheet as much as possible anyway. Other acceptable ways of graphing and comparing icing-related measurements are illustrated in reference [O4].

Table O-3. Effects on Aircraft[3]

Aircraft Effect (AE)	Speed (See Note a)	Power (See Note b)	Climb (See Note c)	Control (See Note d)	Vibration (See Note e)
Level 1	Less than 10 knots loss	Less than 10% increase required	No effect or less than 10% loss	No effect	No effect
Level 2	10-19 knots loss	10%-19% increase required	10%-19% loss rate of climb	No effect	No effect
Level 3	20-39 knots loss	20%-39% increase required	20% or more loss rate of climb	Unusually slow or sensitive response from control input	Controls may have slight vibration
Level 4	40 or more knot loss	Not able to maintain speed	Not able to climb	Little or no response to control input	May have intense buffet and/or vibration

Notes:

a. SPEED: Loss of speed due to aircraft icing. This is based on the indicated airspeed which was being maintained prior to encountering ice on aircraft and before applying additional power to maintain original airspeed.

b. POWER: Additional power required to maintain aircraft speed/performance that was being maintained before encountering icing on aircraft. Refers to primary power setting parameter, i.e., torque, rpm, or manifold pressure.

c. CLIMB: Estimated decay in rate of climb (ROC) due to aircraft icing, example 10 percent loss in ROC, 20 percent loss in ROC, or not able to climb at normal climb speed with maximum climb power applied.

d. CONTROL: Effect of icing to aircraft control inputs.

   Levels 1 and 2. No noticeable effect on response to control input.

   Level 3. Aircraft is slow to respond to control input. Aircraft may feel sluggish or very sensitive in one or more axes.

   Level 4. Little or no response to control input. Controls may feel unusually heavy or unusually light.

e. VIBRATION/BUFFET: May be felt as a general airframe buffet or sensed through the flight controls. It is not intended to refer to unusual propeller vibration (for airplanes so equipped) in icing conditions.

Table O-4 presents a checklist of system and engine operations to be evaluated in icing conditions that can supplement Table O-2. This should be used as a starting point by the applicant. Non-applicable items may be deleted or items may need to be added for a particular design.

[3] This table was devised by the Task 1-B working group under the 1997 FAA Aircraft Icing Plan. It was developed for use with pilot reports (PIREPs) for icing conditions, but it is also suitable as a checklist for icing test flights. The table lists four increasingly worsening levels of effects due to icing conditions on three performance factors (speed, power, and climb capability) and two handling aspects (control and vibration). See reference [O2].

Table O-4. Checklist of Items to be Evaluated in Icing Conditions.

Aircraft S/N: _____ Flight No.: _____ Date: _____

Encounter:	1	2	3	4	Comments
Crew visibility					
Air data					
Airspeed					
Altitude					
Alternate static air					
Temperature					
Stall warning operation					
Autopilot operation					
Electrical load					
Engine operation:					
Normal air or mode					
Alternate air or mode					
Engine cooling					
Propeller IPS operation					
Engine inlet IPS operation					
Ice detection					
Ice detector operation					
AFM ice detection (day)					
AFM ice detection (night)					
Ice Accretions:					
Protected surfaces? (specify)					
Radome?					
Spinner?					
Inlets? (list)					
Side windows?					
Nacelles?					
Pitot probe?					
Temperature probe?					
AOA probe or vanes?					
SW sensor?					
Ice detector probe?					
Antennae (list)					
Instrumentation? (list)					
Aft of IPS?					
Other? (list)					
Ice Shedding:					
Propeller					
IPS normal operation					
IPS delayed activation					
Radome					
Antennae					
Avionics:					
Magnetic heading deviation					
Com/Nav					
Landing gear operation					
Flap operation					
APU operation					
Other (RAT, T/R, etc.)					

O.5 References

O1. "**A Workable, Aircraft-Specific Icing Severity Scheme**", R. Jeck, reprint No. AIAA-98-0094, 36th Aerospace Sciences Meeting (1998), American Institute of Aeronautics and Astronautics, Reston, Virginia 20191-4344.

O2. "**A History and Interpretation of Aircraft Icing Intensity Definitions and FAA Rules for Operating in Icing Conditions**", Richard K. Jeck, FAA Technical Report DOT/FAA/AR-01/91 (2001), FAA Technical Center, Atlantic City, NJ 08405.

O3. "**Ice Accretion and Droplet Impingement Codes**", SAE ARP5903.

O4. "**Icing Design Envelopes (14 CFR-25, 29, Appendix C) Converted to a Distance-Based Format,**" Richard K. Jeck, FAA Technical Report DOT/FAA/AR-00/30 (2000), FAA Technical Center, Atlantic City, NJ 08405.

APPENDIX P. ICE SHEDDING.

P.1 Ice Shedding.

Attention must be given to evaluating the ingestion of ice being shed from protected and unprotected surfaces into the engine(s), in accordance with 14 CFR 23 §.901(d)(2), 14 CFR parts 23 and 25 § .903 and 14 CFR parts 23, 25, 27, and 29 § .1093. Also, the trajectories and energy of shed ice must be evaluated to ensure safe flight of the aircraft, including structural integrity of the airframe and the operation of aircraft systems. When ice is shed during or after an icing encounter, it may create a hazard by entering engine inlet ducts, which would cause structural damage and/or affect the operability of the engine. Ice that is shed could also strike and damage other parts of the aircraft, or block the movement of control surfaces. The aircraft design should consider these hazards and appropriate steps should be taken to prevent unwanted buildup and release of large pieces of ice that could cause hazardous malfunctioning or damage to the engine or aircraft. Maximum ice shedding usually occurs after an ice encounter when the aircraft is flown into ambient temperatures above freezing. Ice may shed from wing and empennage leading edges, windshields, fuselage nose, pitot masts, antennae, propellers, rotors, etc. Experience indicates that small turbine engines are more sensitive to compressor blade damage and adverse engine operation during ice ingestion than are the larger turbine engines. Note that ice shedding that impacts aircraft instrumentation may also have deleterious effects on airplane systems, i.e., AOA vanes and pitot systems.

Analytical assessment of the shed ice trajectories is difficult since the trajectories are influenced by local and downstream flow conditions; the shape, size, and lift-to-drag ratio of the ice fragment; and the tumbling of the ice fragment. Useful information relative to the use of impingement and ice accretion codes for estimating shed ice trajectories is provided in [P1]. Since an analytical model of the entire shedding process is not available at this time, ice shedding is analyzed conservatively to compensate for the inexact nature of the analysis.

The role of droplet impingement and ice accretion codes in ice shedding studies has been to predict the ice shape, size, and mass before the shedding event occurs. Droplet impingement and ice accretion codes cannot predict the frequency of shedding, the shedding event itself, the breakup of ice as it sheds, or the trajectory of shed fragments. The trajectory capability of droplet impingement and ice accretion codes applies only to small particles which are not influenced significantly by gravity and which do not experience aerodynamic forces that are a function of their orientation in the flowfield. In contrast, shed ice fragments are large enough to experience gravitational effects and are highly influenced by aerodynamic forces dependent of their shape, orientation, and rotation at a given moment in time.

The path of ice released from the aircraft is affected by many variables, such as ice fragment shape and mass, aircraft attitude and altitude, airspeed, the airflow around the aircraft, and the manner in which the ice is released. Therefore, it may be difficult on some configurations to show that ice released will not enter into engine inlet ducts or strike and damage aircraft components. A desirable approach for resolving an apparent "ice shedding" problem is to install anti-icing provisions in critical areas.

Shed ice trajectories should be understood as fully as possible prior to flight testing. Also, the differences between shed ice trajectories obtained using a tanker and those obtained under natural icing conditions should be understood prior to accepting tanker testing for evaluating shed ice trajectories. Information relative to the use of icing tankers for evaluating shed-ice trajectories is provided in [P2].

Ice ingested by the engines should not impair the engines' operation and thrust capability. The ice protection of airframe components whose ice accretion affects the integrity of the engines should be considered part of the engine's IPS. Structural damage analyses may be required if ice being shed from forward aircraft components can strike downstream aircraft components. Components including control surfaces and their horns, hinges, control cables, spoilers, and load-bearing structures should be considered.

If anti-icing provisions are not installed in critical ice shedding areas, then investigations should be conducted to show that ice that sheds off the aircraft will not cause an unsafe condition. "Ice shedding" investigations should be made during and after ice encounters. Sufficient encounters in all intended operational conditions should be made to ensure there is no hazard associated with the shedding of ice. In addition to the usual measurements and observations made during ice encounter tests, the following additional instrumentation and/or observations are suggested:

- Motion pictures to record the trajectory of ice released from the aircraft
- A data acquisition system for turbine-engine-powered aircraft to record EGT, EPR, and rpm, in order to detect adverse effects on engine operation
- Visual examination of the aircraft for damage before and after ice encounters, especially in the area of the engine compressor and inlet

In addition, a damage analysis should consider that the most critical ice shapes will shed and impact the areas of concern.

P.2 References

P1. "Ice Accretion and Droplet Impingement Codes," SAE ARP5903.

P2. **"Airborne Icing Tankers,"** SAE ARP5904.

APPENDIX Q. WINDSHIELD ICE PROTECTION.

Testing should verify the design of the windshield IPS. Inner and outer windshield surface temperature surveys of the protected areas should be performed to verify design thermal analyses. The thermal analyses should substantiate that the surface temperatures are sufficient to maintain anti-icing capabilities without causing structural damage to the windshield. An evaluation of the visibility, including optical distortion effects, should be made for day and night operations. In addition, the size and location of the protected area should be reviewed for adequate visibility, especially for approach and landing conditions. A probable single failure of a transparency heating system should not adversely affect the integrity of the airplane cabin or create a potential fire hazard. The applicant should develop safety analysis per AC 23.1309-1C and AC 25.1309-1 guidance to show that windshield IPS meets the reliability and safety requirements.

APPENDIX R. ICE SHAPES.

R.1 Protected Surfaces

R.1.1 Pre-Activation Ice Roughness

Ice accretion roughness on unprotected and protected aircraft surfaces prior to effective operation of the IPS using recommended procedures should be considered in demonstrating safe aircraft flight in icing conditions, as discussed in Section 6.2 – Safe Flight in Icing Conditions. This surface roughness may seem small, but the resulting aerodynamic effects may be significant. Also, since safe flight considerations may require adjustments to the uncontaminated aircraft stall protection and other systems, the scheduled performance and maneuvering capability of the uncontaminated aircraft may be affected. See Advisory Circulars 23.1419-2B, 25.1419-1, 27-1B, and 29-2C for specific information. Safe operation considerations for pre-activation ice accretion should include adequate stall warning and safe flying qualities at and above stall warning. Icing conditions exposure times should include delay times associated with the detection of ice accretion, flight crew reaction time to activate the IPS using recommended procedures, and the time required for the IPS to become effective.

Pre-activation ice accretion roughness will vary with the aircraft's IPS design, the aircraft's design, and the ice protection operating procedures and is configuration dependent. Therefore, the applicant should determine and substantiate the pre-activation ice roughness for the specific model design. The selected roughness should consider the time required for the IPS to become fully effective and the icing condition that results in the most critical effects on airplane flying qualities. Figures R-1, R-2, and R-3 illustrate pre-activation ice surface roughness observed on the leading edge of a hybrid NACA 23012 2-dimensional icing wind tunnel model (approximating a 72-inch chord airfoil). Note, the sand roughness of the pre-activation ice can be gauged by the grids formed by the one-inch apart chordwise lines and the two 1 1/4 inch spanwise lines along the leading edge of the model. Castings of the model surface roughness shown in R-1 and R-2 are available from the FAA William J Hughes Technical Center, Organization AAR-421. Figure R-1 illustrates the surface roughness that may accrete during the time required for an ice detector to detect ice accretion (11 seconds for the first deicing cycle of a magnetostrictive type ice detector) in maximum continuous icing conditions and an additional 30 seconds to allow the pilot to initiate recommended anti-icing procedures. The applicant should provide the pre-activation ice accretion roughness for his aircraft design to the FAA for their approval.

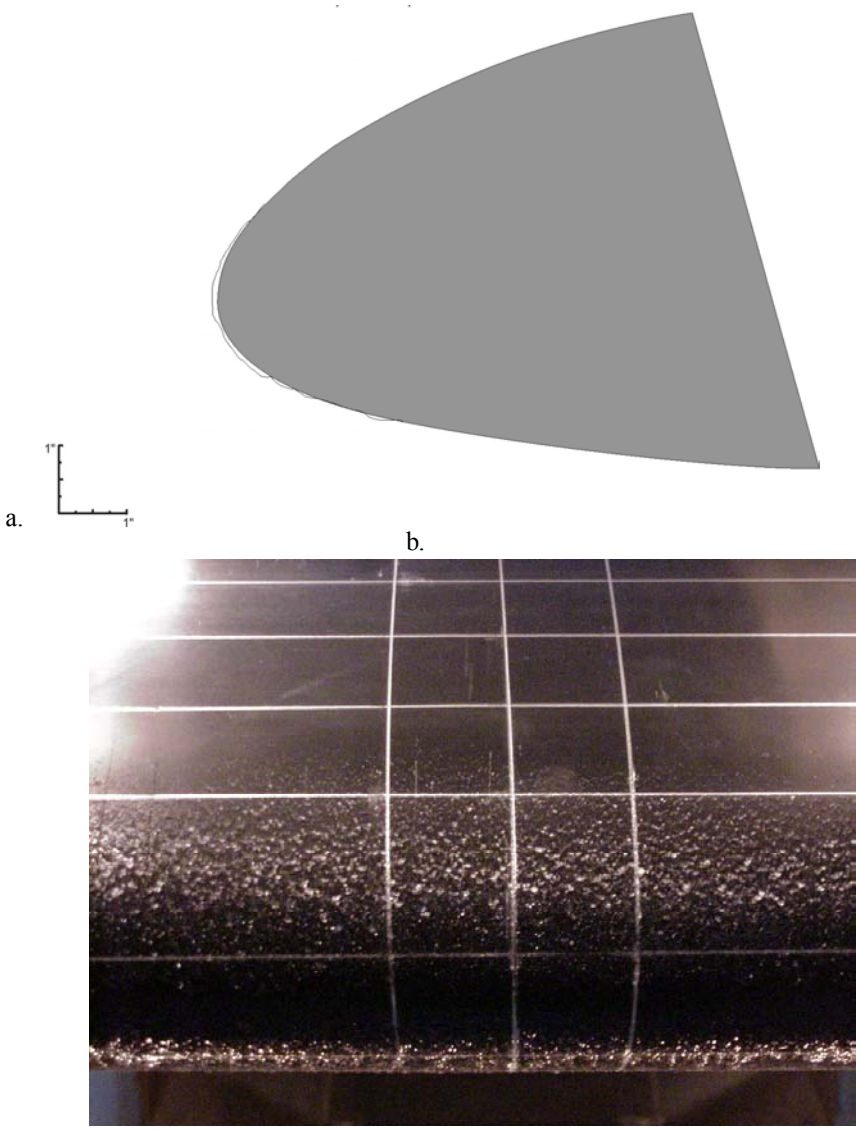

Figure R-1. Hybrid NACA 23012 two-dimensional (simulating a 72-inch chord airfoil) model leading edge ice roughness prior to activation of the ice protection system, allowing 11 seconds for an ice detector alert and 30 seconds for the flight crew to activate the ice protection system, in 14 CFR part 25, Appendix C continuous maximum icing conditions. (Static temperature = 14°F, LWC = 0.45 g/m^3, MVD = 20 micrometers, Spray time = 41 sec., Tunnel airflow speed = 195 mph, Model AOA = 4°.) [R1]

Figure R-2 illustrates the model's leading edge pre-activation surface roughness that occurred during exposure to intermittent maximum icing conditions (three seconds for the first cycling of the ice detector and 30 seconds for the pilot to initiate recommended procedures). Figure R-3 illustrates the model's leading edge surface roughness that followed visual observation of ¼ inches of ice accretion and an additional 30 seconds of exposure to maximum continuous icing conditions to allow for the pilot to initiate recommended deicing procedures. Note that more than one deicing cycle of an ice detector can be selected to avoid nuisance ice detection warnings or activation of the IPSs. Also, the use of two minutes for flight crews to recognize icing conditions and initiate recommended procedures is considered acceptable for propulsion IPSs. When determining the delay time for pilots to initiate recommended ice protection procedures, consideration should be given to the means provided to the flight crews for detecting the first accretion of airframe icing and the flight

crew workload. The time required for the IPS to become fully effective varies with each system, e.g., the time for thermally protected surfaces of a specific aircraft model to reach the design temperature. For IPSs that activate components sequentially, the time required for activation of the complete system should be considered as part of the pre-activation exposure to icing conditions.

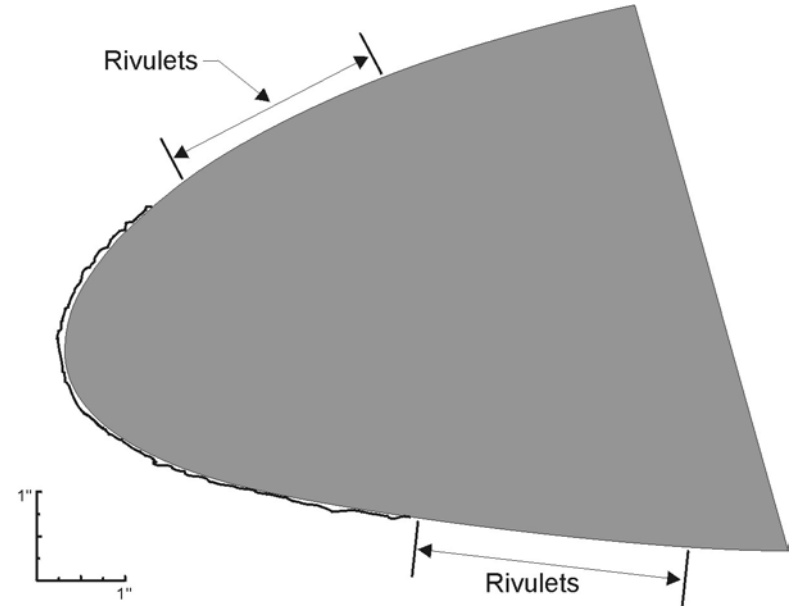

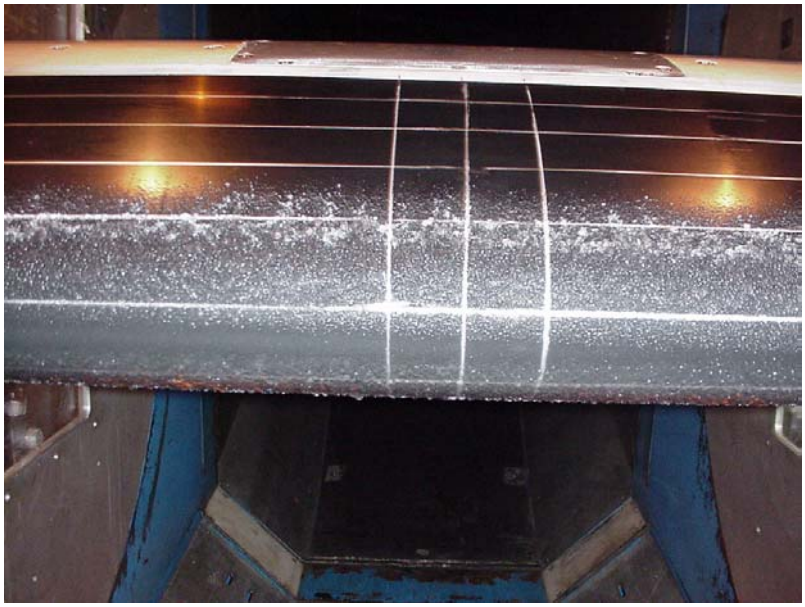

Figure R-2. **Hybrid NACA 23012 two-dimensional (simulating a 72-inch chord airfoil) model leading edge ice roughness prior to activation of the ice protection system, allowing 3 seconds for an ice detector alert and 30 seconds for the flight crew to activate the ice protection system, within 14 CFR part 25, Appendix C intermittent maximum icing conditions. (Static temperature = 14 °F, LWC = 1.95 g/m3, MVD = 20 micrometers, Spray time = 33 sec., Tunnel airflow speed = 195 mph, Model AOA = 4°.) [R1]**

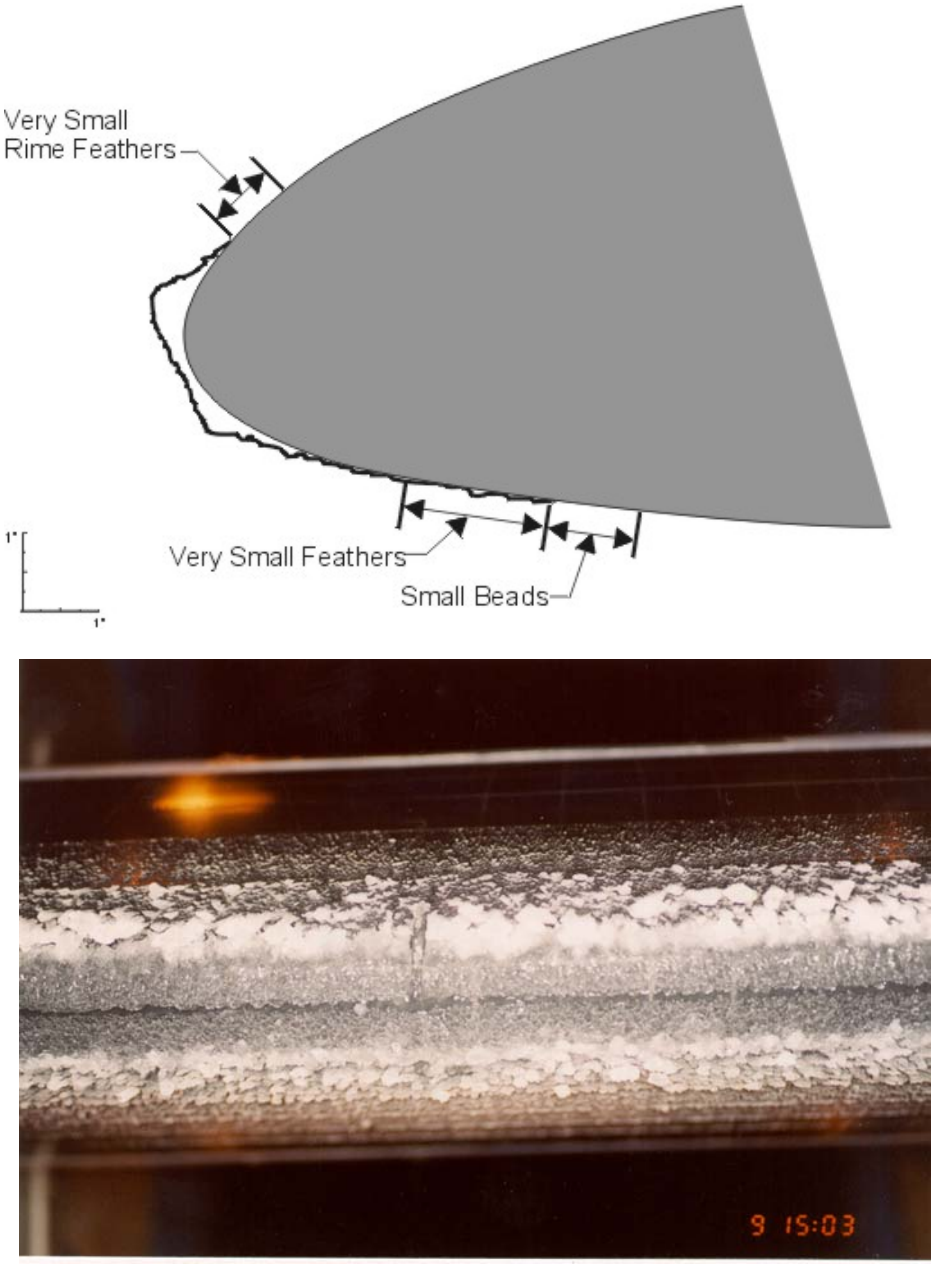

Figure R-3 **Hybrid NACA 23012 two-dimensional model (simulating a 72-inch chord airfoil) leading edge ice roughness prior to activation of the ice protection system, assuming flight crew observation of ¼ inches of ice and 30 seconds for the flight crew to activate the ice protection system, in 14 CFR part 25, Appendix C continuous maximum icing conditions. (Static temperature = 14° F, LWC = 0.45 g/m^3, MVD = 20 micrometers, Tunnel airflow speed = 195 mph, Model AOA = 4°.) [R1]**

R.1.2 Intercycle Ice Roughness

For continued operation of the deicing system, the IPS may be activated based on visual observation of a recommended monitored surface ice thickness, typically ranging from ¼ to 1½ inches. Figure R-3 illustrates the surface roughness that may be expected following visual observation of ¼ inch of ice accretion and an additional 30 seconds of exposure to maximum continuous icing conditions to allow the pilot to activate the deicing IPS. Since the cycling sequence time may be relatively lengthy for some aircraft designs, ice accreted on the protection surfaces during the cycling sequence should also be considered. Other mechanical systems are expected to have different intercycle ice accretion characteristics. It should be shown that asymmetric intercycle ice accretion resulting from sequential operation of the elements of the IPS does not result in unsafe aircraft operations. Alternatively, continuous operation of a deicing system may be automated based on pre-selected time intervals.

Intercycle ice roughness should be determined and substantiated by the applicant for the protected components of their model design.

Figures R-4(a) and R-4(b) illustrate intercycle ice roughness obtained on a wind tunnel model using three-minute and one-minute intervals between cycling of the deicing boots in typical icing conditions. Note, the texture of the intercycle ice can be gauged by the grids formed by the one-inch apart chordwise and spanwise lines shown in the photographs. Castings of the intercycle ice shown in Figures R-4(a) and R-4(b) are available from the FAA William J Hughes Technical Center, Organization AAR-421.

For smaller surfaces, such as the horizontal stabilizers of regional air transports, Figure R-5 illustrates intercycle ice roughness obtained on a 2-dimensional 36-inch NACA 23012 airfoil wind tunnel model using three- and one-minute intervals between cycling of the deicing boots.

Figure R-6 illustrates that the intercycle ice roughness shown in Figures R-4 and R-5 compare favorably with that observed during flight. The wing leading edge deicing boots shown in Figure R-6(a) were cycled just prior to landing after the aircraft had experienced heavy icing conditions. Figure R-6(b) is a photograph, obtained in flight during a revenue operation, of wing leading edge deicing boots intercycle ice accretion. The losses in maximum lift, maximum lift AOA, and increases in drag at operational angles-of-attack and as maximum lift is approached underscore the need to properly model normal operation protection surface roughness when demonstrating performance and handling qualities in icing conditions.

Aerodynamic effects of intercycle ice surface roughness can be significantly adverse. Figure R-7 illustrates the aerodynamic effects of intercycle ice surface roughness obtained during icing wind tunnel and during high Reynolds number wind tunnel testing of a two-dimensional, 36-inch NACA 23012 airfoil. Texture of the intercycle ice is available from castings of the intercycle ice shown in Figure R-5(b) (these castings are available from the FAA William J Hughes Technical Center, Organization AAR-421). Data shown in Figure R-8 illustrate that the aerodynamic effects of uniformly distributed roughness, such as carborundum grit, do not result in aerodynamic effects similar to those of the tested intercycle ice surface roughness. The applicant should validate the use of uniformly distributed roughness to simulate intercycle ice shapes.

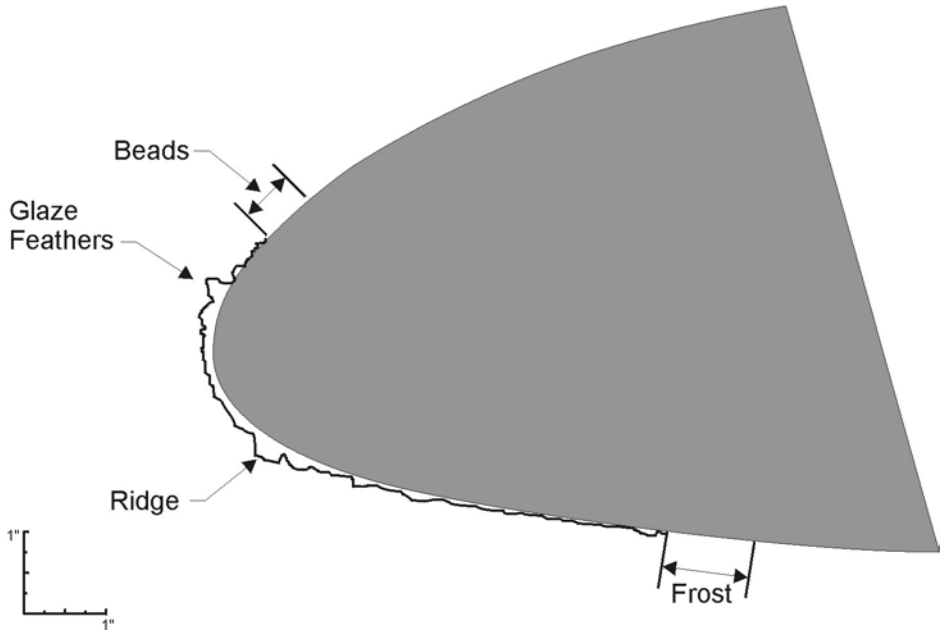

Figure R-4(a) Hybrid NACA 23012 two-dimensional (simulating a 72-inch chord airfoil) model intercycle ice prior to third cycle of pneumatic deicing boot, with a 3-minute boot cycle interval, in 14 CFR part 25, Appendix C maximum continuous icing conditions. (Static temperature = 14° F, LWC = 0.45 g/m^3, MVD = 20 micrometers, Spray time = 6:11 min., Boot cycle interval = 3 min., Tunnel airflow speed = 195 mph, Model AOA = 4°.)

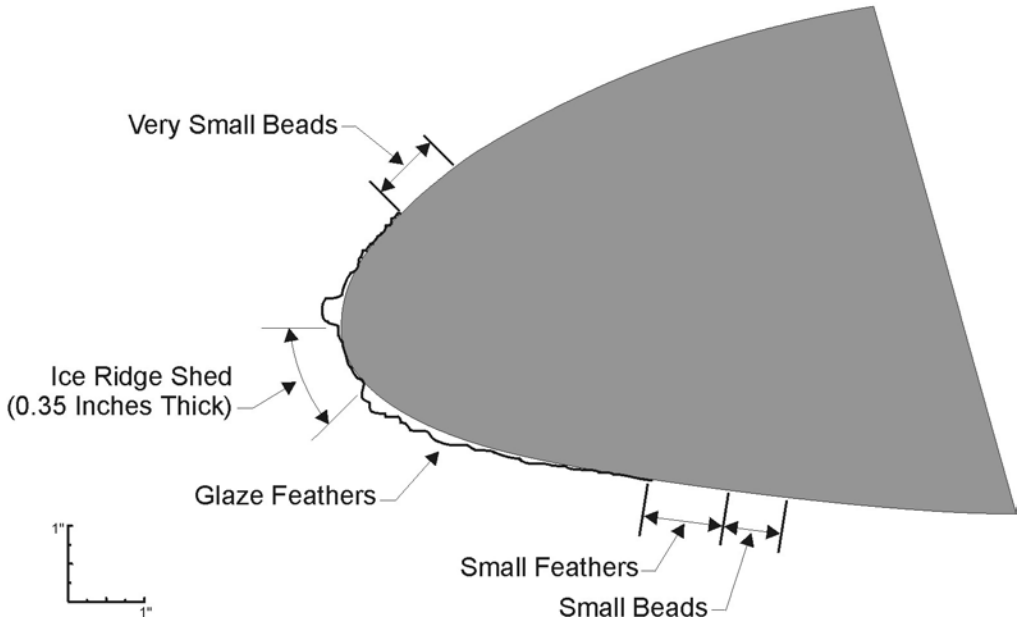

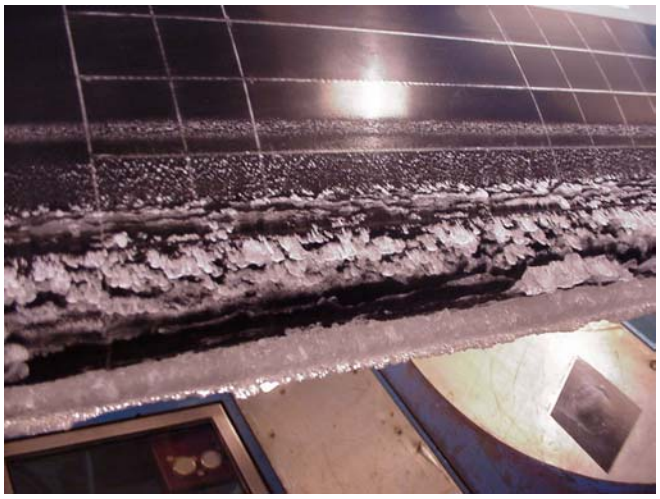

Figure R-4(b). Hybrid NACA 23012 two-dimensional (simulating a 72-inch chord airfoil) model intercycle ice prior to sixth cycle of pneumatic deicing boot, with a 1-minute boot cycle interval, in 14 CFR part 25, Appendix C maximum continuous icing conditions. (Static temperature = 14° F, LWC = 0.45 g/m^3, MVD = 20 micrometers, Spray time = 6:11 min., Boot cycle interval = 1 min., Tunnel airflow speed = 195 mph, Model AOA = 4°.)

Figure R-4. Typical surface roughness on the leading edge of a NACA 23012 resulting from normal operation of wing pneumatic deicing boots. [R1]

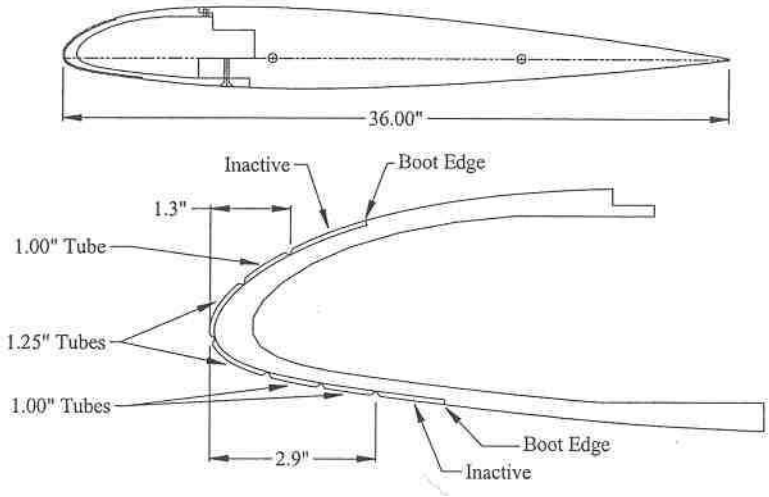

Figure R-5(a). Ice protection design (pneumatic deicing boots) for the NACA 23012 airfoil tested to examine intercycle ice accretion.

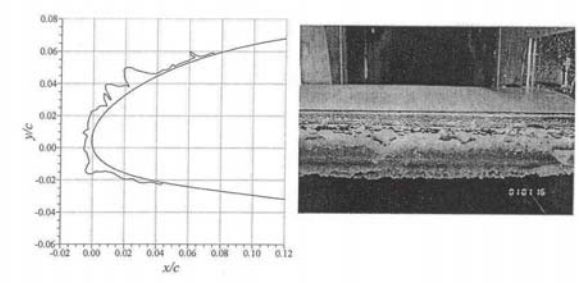

Ice shape 290

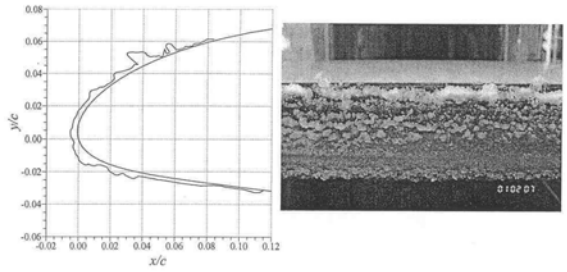

Ice shape 296

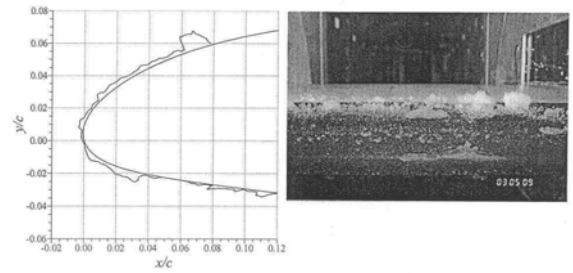

Ice shape 312

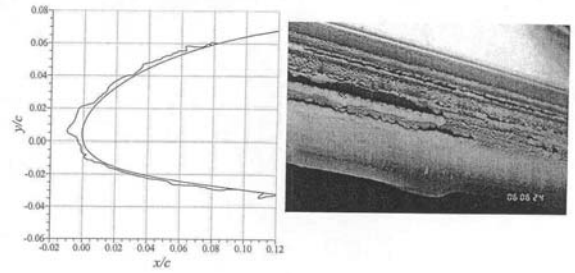

Ice Shape 322

Ice Shape	Angel of Attack (deg.)	Droplet MVD (µm)	Static Temp. (deg. F)	LWC (g/m^3)	Spray Time (min.)	Boot Cycle Period (min.)
290	0	20	14	0.45	12	3
296	0	20	21	0.65	12	3
312	0	40	21	0.25	12	3
322	0	40	-4	0.40	3	1

Figure R-5(b). Icing wind tunnel intercycle ice accretions obtained on the Figure R-5(a) model.

Figure R-5. Intercycle ice roughness obtained on a 2D 36-inch NACA 0012 airfoil wind tunnel model.

Figure R-6(a). Residual ice following cycling of the deicing boots prior to landing during an inflight icing encounter.

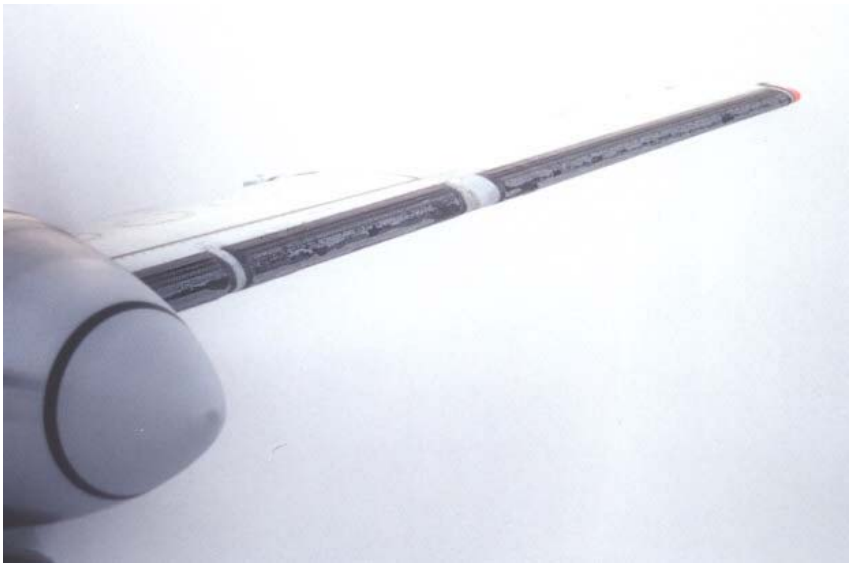

Figure R-6(b). Wing leading edge deicing boots intercycle ice accretion observed during revenue service

Figure R-6. Observed wing leading edge deicing boots residual and intercycle ice accretions.

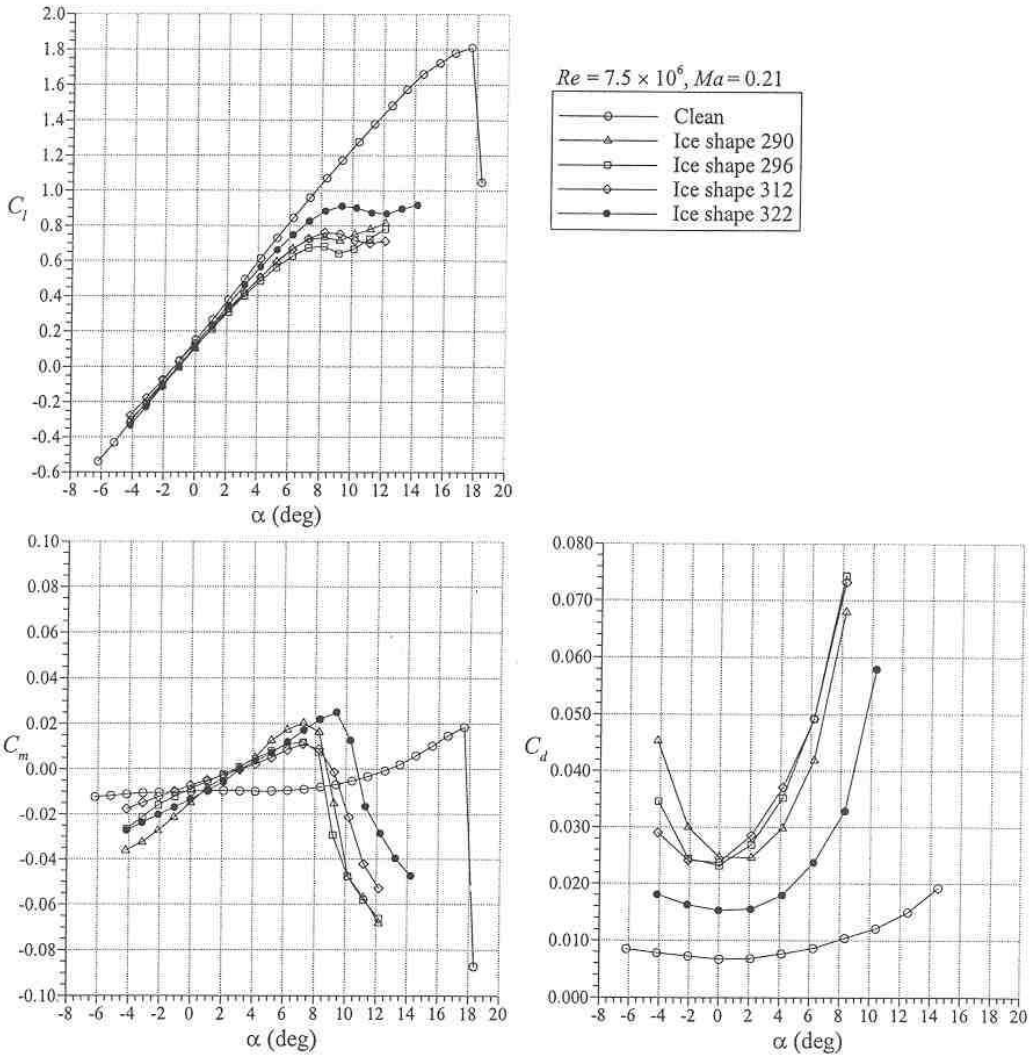

Figure R-7. Aerodynamic effects due to deicing system intercycle ice shapes for a 2D 36-inch NACA 23012 airfoil wind tunnel model at a Reynolds number of 7.5×10^6.

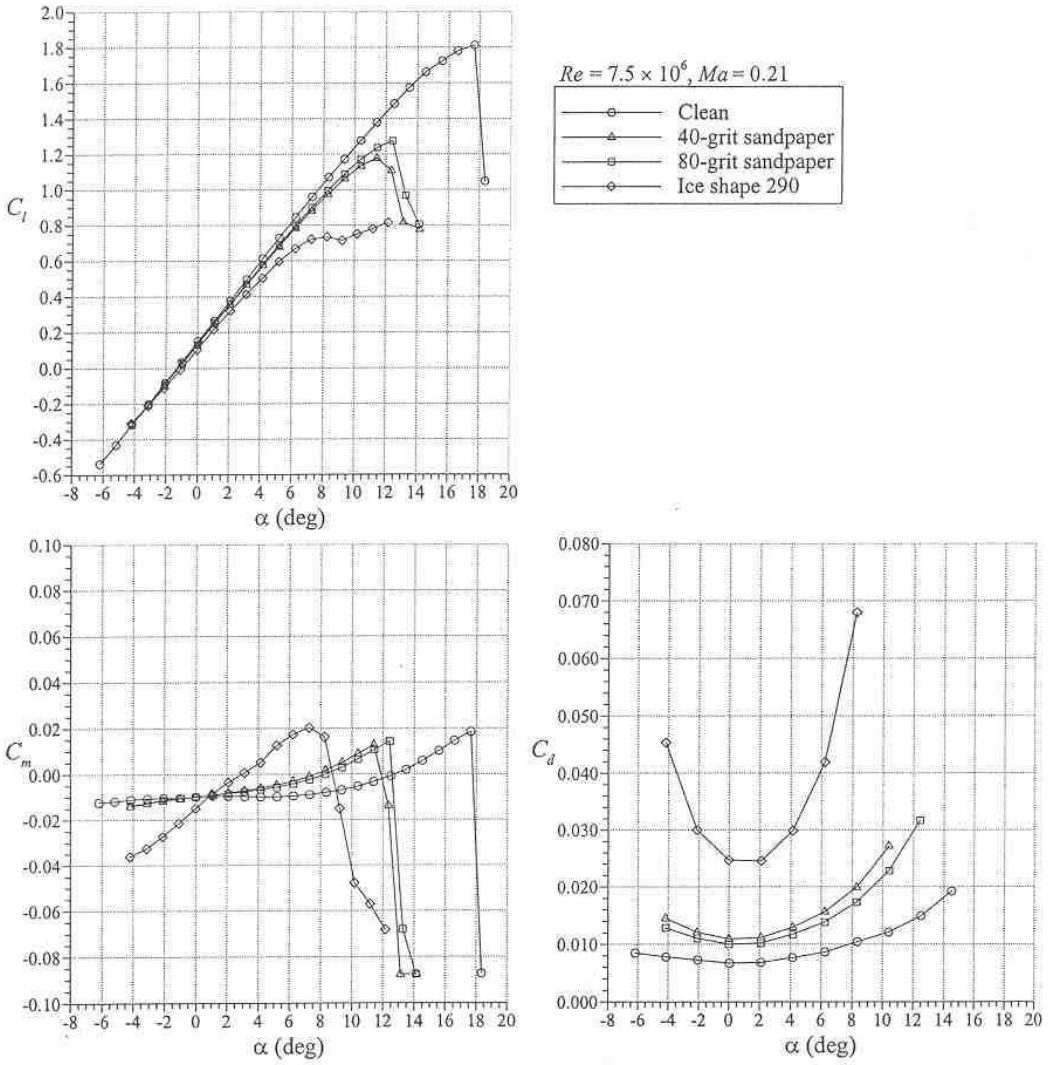

Figure R-8. Performance degradation due to distributed roughness along the leading edge of NACA 23012 airfoil (c = 36 inches, Re = 7.5x10^6, M = 0.21) [R2].

R.1.3 Runback Ice

Water not evaporated by a thermal IPS and unfrozen water during near-freezing conditions—or when the freezing fraction (n) is less than 1.0—may run aft of the ice protection surfaces and form runback ice.

Figure R-9 illustrates runback ice obtained on a 36-inch NACA 0012 duty airfoil model after a 5-minute exposure to icing conditions. The model was equipped with an electrothermal IPS operating in the running-wet mode (surface temperature of approximately 50°F with an icing wind tunnel static temperature of 0°F). The tunnel icing conditions were mixed-phase, with 20 μm droplets at an LWC of 0.35 g/m^3 and with shaved ice particles at an IWC of 0.35 g/m^3. Mixed phase icing conditions are not specifically defined within Appendix C. However, the runback accumulations shown have similar characteristics to those produced by Appendix C liquid phase conditions.

Figure R-9. Lower surface runback ice on a 36-inch NACA 0012 airfoil model, equipped with an electro-thermal ice protection system operating in a running-wet mode (protection surface temperature maintained at approximately 50 °F), following a 5 minute mixed-phase icing exposure. (Static Temperature = 0 °F, LWC = 0.35 g/m^3, MVD = 20 micrometers, IWT (shaved ice) = 0.35 g/m^3, Tunnel airflow speed - 120 mph, Model AOA = 0°.)

Computer codes may be unable to estimate the characteristics of the runback water or the resultant ice shapes, however, some codes may be able to estimate the mass of the runback ice. Until this code capability is developed and validated, runback ice should be determined empirically. However, once this code capability is established, results from computer programs should be substantiated by experimental observations from natural icing tests, icing tanker tests, or icing wind tunnel tests.

Runback ice should be determined and substantiated by the applicant for the protected components of their model design. The effects of runback ice resulting from a 45-minute hold should be considered when demonstrating the safe flight of the aircraft during icing conditions. For thermal systems that operate with runback under holding conditions, consideration should be given to the potential ice shedding and ingestion of runback ice from surfaces in front of engines or engine inlet IPS runback ice.

R.2 Unprotected Surfaces

Aircraft will typically have surfaces on which ice will accumulate and for which no ice protection is provided. Safe operation of the aircraft in icing conditions must be demonstrated with these surfaces unprotected against ice accretion. (See section 6.1 – Applicable Regulations.)

Unprotected surfaces' ice shapes may be determined by tests in measured natural icing or predicted by artificial icing (icing tanker) flight tests, icing wind tunnel tests, computer codes, and other analytical methods validated by test experience. Flight tests in measured natural icing conditions are required by 14 CFR parts 23, 25, 27,

and 29, § .1419 in part to verify the ice protection analyses and to check for icing anomalies. Therefore, predicted ice shapes must be verified by flight tests in measured natural icing conditions. It is not intended that natural icing flight tests validate all aspects of predicted ice shapes, as the probability of finding specific, critical conditions may not be feasible (see Appendix M). The intent is to corroborate the general physical characteristics and location of the artificial ice shapes, and in particular, their effect on airplane handling characteristics.

R.3 Ice Protection System Failure Ice Shapes

It may or may not be necessary for an aircraft to exit icing conditions following failure of the IPS. The following describe IPS failure ice accretion scenarios:

- If the IPS failure condition is annunciated and if AFM procedures require the aircraft to exit icing conditions, the ice accretion on normally protected surfaces should be that resulting from normal operation of the IPS up until the annunciated failure plus that which would accrete during the exiting maneuver.

- If the IPS failure condition is annunciated and the AFM procedures do not require the aircraft to exit the icing conditions, ice accretion on protected surfaces for which ice protection has failed should be that which would accrete on an unprotected surface.

- If the IPS failure condition is not annunciated, ice accretion on normally protected surfaces should be that which would accrete on an unprotected surface.

When the aircraft is required to exit icing conditions, ice on normally protected surfaces where ice protection has failed may be selected to be half of that which would accrete on an unprotected surface. Alternatively, if the IPS failure is annunciated, the ice that would accrete on an unprotected surface during the time required to exit the icing condition may be selected. The time required to exit the icing conditions must be calculated conservatively; the appropriate Directorate needs to be consulted. For airplanes, the time to exit the icing condition may be selected as half of a 45-minute hold, or as substantiated by the applicant. The time to exit the icing conditions for a rotorcraft is 15 minutes as presented in AC 29-2C. For a failed IPS, ice accretion on unprotected surfaces should be unaffected and expected to accrete as described in R.2 – Unprotected Surfaces. See R.2 – Unprotected Surfaces for means of determining ice shapes for unprotected surfaces.

Determining if an aircraft is required to exit icing conditions should be based on results of the system failure and failure modes and effects analysis required by 14 CFR parts 23, 25, 27, and 29 § .1309. If continued flight in icing conditions is selected, the aircraft must be demonstrated to be capable of safe flight, as described in 6.2 – Safe Flight in Icing Conditions. Simulated ice shapes developed to evaluate the aircraft's performance and handling qualities should replicate the allowable failures of the IPS. If the aircraft is required to exit icing conditions, the aircraft must demonstrate the capability of safe continued flight and landing, and appropriate procedures should be included in the AFM. For guidance relative to means of demonstrating safe flight following failure of the IPS that requires exiting the icing condition, see: AC 23-8A and 23-8A, Change 1; AC 23.1419-2B; AC 25.7A; AC 25.1419-1; AC 27-1B; and AC 29-2C.

R.4 Critical Ice Shapes

R.4.1 Considerations for Critical Ice Shapes

A critical ice shape may be defined as the aircraft surface ice shape formed within icing conditions, defined by 14 CFR part 25 or part 29, Appendix C, that results in the most adverse effects for specific flight safety requirements. For example, the critical ice shape may differ for different flight safety requirements, e.g., stall speed, climb, aircraft controllability, control surface movement, control forces, air data system performance,

"artificial feel" adjustments, ingestion and structural damage from shed ice, engine thrust, engine control, and aeroelastic stability.

Critical ice shapes may vary with aircraft configuration and flight phase. An aircraft surface ice shape may be determined to be critical for all other flight safety considerations, configurations, and flight phases. Critical ice shape determination also includes consideration of ice shapes that have an unsatisfactory effect on the aircraft's aeroelastic stability (14 CFR parts 23, 25, 27, and 29, § .629) and shed-ice ingestion related to engine operation, control, and ice protection (14 CFR part 23§ .901(d)(2), 14 CFR parts 23 and 25 § .903 (which require compliance with 14 CFR part 33 § .77), 14 CFR part 33 § .68, and 14 CFR parts 23, 25, 27, and 29 § .1093).

Flight testing with the critical ice shapes can be dangerous if approached with insufficient caution. To avoid extensive flight testing, the simulation of the most critical unprotected and protected surface ice shapes and surface roughness may be used as a means to demonstrate compliance with the applicable 14 CFR parts 23, 25, 27, and 29, Subpart B requirements to show safe flight in icing.

If a single critical ice shape configuration cannot be established, each critical ice shape should be tested in the appropriate phase-of-flight configurations to investigate the aircraft's controllability, maneuverability, stability, performance, trim, and stall characteristics. Generally, for large turbojet air transports with large thrust margins, emphasis is placed on ice shapes that are critical relative to handling qualities, with conservative estimates of performance effects being taken into account. All flight testing should be accomplished at the most critical weight, center-of-gravity, flap, and gear configuration for the aircraft characteristic of interest.

Determination of critical ice shape configurations is not necessarily straightforward and may require engineering judgment. The aircraft critical ice configuration should include expected ice accretion on all surfaces, protected and unprotected (including flow control devices such as vortex generators, stall strips, vortilons, and fences), to determine the full impact on airplane flying and structural qualities. Phases of flight to consider include those in which ice accretion may occur and those for which ice accretion may continue to exist after exiting conditions conducive to icing. Consideration of the ice accretion effects on the aircraft should include the following:

- Lift, including maximum lift
- Drag
- Pitching moments
- Control forces
- Control surface movement
- Freezing of critical seals
- Ice ridges aft of protection surfaces
- Runback ice
- Vibration and aeroelastic stability
- Stall warning
- Stall characteristics
- Power

- Air induction inlet airflow
- Stability
- Controllability
- Trim
- Control surface aerodynamic balance
- Maneuverability
- Horizontal stabilizer and elevator stall
- Vertical stabilizer and rudder stall
- Wake effects on engine operability and downstream aircraft components and systems
- Engine operability and aircraft structural damage resulting from shed ice

The applicant should select the critical ice shape configuration(s) and provide substantiation that the selected ice shape configuration is most critical for the aspect of flight safety considered. Selection of the ice shape and ice shape features typically requires surveying ice shapes that may accrete on a surface or component within the applicable icing conditions. Critical ice shape candidates are selected from this survey, with an understanding that an ice shape that is critical for a surface or component relative to a flight safety consideration may not be that of an unprotected surface that may have the largest and most aerodynamically intrusive ice accretion. Surfaces and components are protected if their protection is considered critical relative to safe flight. Therefore, pre-activation ice accretion roughness, protection surface intercycle ice accretion roughness, runback ice, or thin, rough ice accretions on the horizontal stabilizer (resulting from pre-activation ice, intercycle ice, or from being an unprotected surface), along with the expected ice accretion on unprotected surfaces and components, should be considered.

Ice shapes capable of being produced during applicable icing conditions and their characteristics can be determined by flight in natural or artificial (icing tanker) icing conditions, icing wind tunnel tests, ice accretion codes or analysis methods, or by combinations of the different methods. It should be noted that 14 CFR § 25.1419 requires flight tests in measured natural icing conditions to verify the ice protection analysis, to check for icing anomalies, and to demonstrate that the IPS and its components are effective. When icing tankers, icing wind tunnels, and/or ice accretion codes and analytical methods are used, comments pertaining to the use of these icing simulators contained in R1 – Protected Surfaces and R2 – Unprotected Surfaces should be considered.

Inflight icing accident investigations and experience suggest that glaze and high intensity icing conditions during descent may result in the most aerodynamically hazardous ice shapes. Glaze icing conditions will exist at near-freezing temperatures (approximately -5° C or warmer) and the largest ice mass will occur at conditions of maximum water catch. Hazardous ice accretions may also occur at colder mixed and rime ice conditions for intercycle ice and for running-wet thermal IPSs.

Experience from previous certifications of similar aircraft designs may be used as guidance for determining the icing conditions that produce candidate critical ice shapes.

Unprotected critical surface ice shapes should reflect the icing exposure time interval associated with the respective phase of flight. For the holding configuration, the 45-minute holding period should be considered.

Guidance material, such as that of the JAA ACJ 25.1419, states that from service experience the amount of ice on the most critical unprotected main airfoil surfaces need not usually exceed a pinnacle height of three inches in a plane in the direction of flight [R3].

Service experience often referenced was described in a 1962 airframe manufacturer's magazine article that discussed elimination of the B707/720 model airplanes' horizontal and vertical stabilizers leading edge ice protection [R4]. The magazine article provided an analysis of a "maximum possible ice (based on CAR icing conditions envelopes)" mission profile that resulted in a maximum ice shape of 3.31 inches, following:

- A dispatch hold of 10.4 minute at an airspeed of 250 KTAS,
- Climb of 4.5 minutes at an airspeed of 290 KCAS,
- Cruise at an altitude of 15,000 feet for 22 minutes at an airspeed of 360 KIAS,
- A destination hold of 31 minutes at 15,000 feet with an airspeed of 250 KTAS.

Flight test demonstrated that these Boeing airplane models were not hampered by three-inch simulated ice shapes, relative to minimum control speeds, control capability, or stability. The article only addressed the horizontal and vertical stabilizers of the B707/720 models and also stated that the analysis was applicable only to turbine powered airplanes. The 3.31 inches analysis ice shape and the flight test three-inch ice shape discussed in the magazine article may lead to the conclusion that service experience shows that the ice on the most critical unprotected main airfoil surfaces need not exceed a pinnacle height of three inches. Certification experience has shown that pinnacles heights on the most critical unprotected surfaces may exceed three inches, such as on the unprotected leading edges of the horizontal or vertical stabilizers or the wing of airplanes smaller in scale than the Boeing 707.

Also, the magazine article's combination of a dispatch takeoff hold and a destination hold may be related to the above 45-minutes destination hold (based on operational fuel requirements) ice shape guidance."

Pre-activation and intercycle ice shapes are aircraft design–sensitive and should be determined by the applicant. However, information in Section R.1.1 – Pre-Activation Ice Roughness and Section R.1.2 – Intercycle Ice Roughness may be used as guidance. Castings of these ice accretions, which may be used as a guide for fabricating simulated ice roughness, are available at the FAA William J. Hughes Technical Center. For larger ice shapes, which would accrete on unprotected surfaces, the ice shape surface texture should either reflect the empirically determined ice shape texture or should be approximately 3 mm in height with a particle density of 8 to 10 per cm^2. Thin, rough layers of ice, commonly called "sandpaper ice" should reflect empirical results. (Carborundum paper no. 40 has been used during certification for ice contaminated tail stall). However, use of the 40-grit carborundum paper to simulate intercycle ice roughness should be substantiated (as discussed in section R.1.1 – Pre-Activation Ice Roughness and section R.1.2 – Intercycle Ice Roughness).

Runback ice and ice ridges that may occur aft of deicing or running wet protection surfaces may form critical ice shapes. These critical shapes should be determined empirically, using icing tankers or icing wind tunnels, until the capability of an ice accretion code or analysis method has been validated to accomplish this task.

Determining the critical aircraft ice shape configuration requires integrating knowledge about all the aircraft's surfaces' and components' critical ice shapes into one overall configuration. The integration process may reveal that the critical ice shape for one surface may not be consistent with the development of critical ice shapes on other surfaces. For example, sandpaper ice roughness on the horizontal stabilizer may be critical for contaminated tail stall testing, whereas the wing's extended holding and intercycle ice configurations may be critical for airplane performance and handling qualities. Also, propeller ice accretion may be considered necessary for demonstrating stall recovery and drag for aircraft with low power margins, but may be considered insignificant for demonstrating other safe flying qualities.

Simulated critical ice shapes may be used to demonstrate safe flight in icing conditions. To minimize the number of configurations necessary to demonstrate safe flight in icing with simulated ice shapes, the applicant should demonstrate that the selected configurations are most critical. Without applicable information from an appropriate, certificated predecessor aircraft model and for other than the simplest aircraft configuration, wind

tunnel testing at the appropriate Reynolds and Mach numbers or a validated Navier-Stokes full-configuration CFD analysis may be necessary (see the discussion of CFD codes in Section R.4.2 – Aerodynamic Considerations for Determining Critical Ice Shapes). Also, when incrementally adjusting flight test data for other critical ice shape considerations by using wind tunnel data, like drag, particular attention should be given to the effects of Reynolds and Mach number on those increments. (Ice accretions may be difficult to replicate on a small scale, and the scale of the ice accretion relative to the model's boundary-layer height may differ from that at flight Reynolds number. Also, scaling the ice shape roughness may be difficult.)

Three-dimensional characteristics of critical ice shapes may be simulated for flight as long as sufficient empirical information is provided to validate the simulated shapes. For surfaces whose chord and leading edge shape changes significantly across the span of the unprotected surface, the critical ice shape may reflect the effects of the varying surface geometry on ice accretion. A three-dimensional (3D) critical ice shape may be created for testing by first lofting two-dimensional critical ice shapes at a sufficient number of span-wise locations and then applying appropriate surface texture, as discussed above, to the 3D surface created by lofting. Low Reynolds number wind tunnel test data, shown in Figure R-10, for a straight, two-dimensional model indicates for the airfoil, ice shape, and conditions tested, that a continuous ice shape provides conservative aerodynamic effects relative to those that are segmented spanwise in order to simulate observed variations in ice accretion.

The use of simulated ice shapes suspected of being the worst or the use of devices that render the surface aerodynamically ineffective should be critically reviewed. The objective of demonstrating safe flight is to have the aircraft behave as if it has experienced the applicable icing environment. Arbitrarily-developed aircraft surface flow conditions may not properly replicate flying qualities of the aircraft with critical ice shapes accreted in natural icing conditions.

Simulated critical ice shapes used to demonstrate safe flight should include collateral icing that may occur on aircraft surfaces. As seen in Figure R-6(a) for an aircraft that had experienced highly intense icing prior to landing, the collateral icing can be significant. Ice accretion codes may fail to predict icing that may accrete at aircraft surface discontinuities. Although drag may be the most significant effect of the collateral ice, these ice accretions should be addressed when demonstrating safe flight (14 CFR §§ 23.65, 23.67(e)(2), 23.67(e)(3), 23.75, 23.77, 25.119, 25.121, and 25.123).

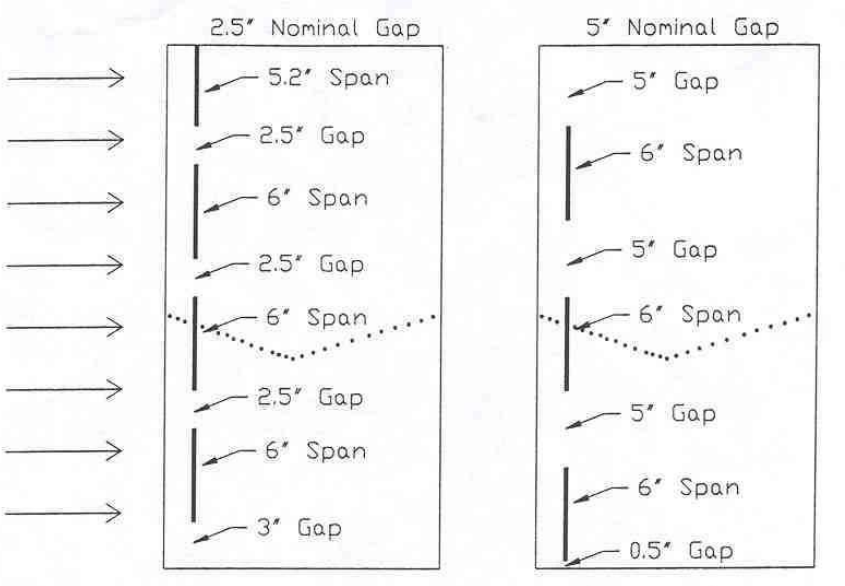

Figure R-10(a). Configurations of segmented 0.25 inch forward-facing quarter-round simulated ice shapes on the upper surface of an 18-inch chord NACA 23012m airfoil two-dimensional model.

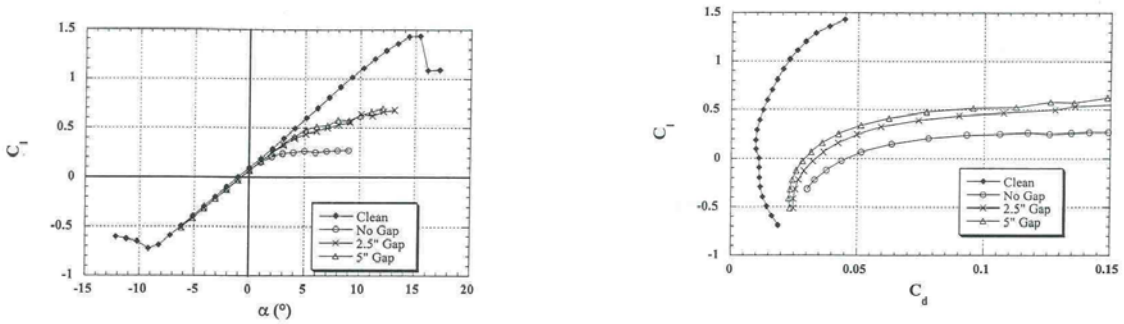

Figure R-10(b). Aerodynamic effects of continuous and segmented 0.25 inch forward-facing quarter-round simulated ice shapes on the upper surface of an 18 inch chord NACA 23012m airfoil two-dimensional model (Re = 1.8×10^6, M=0.185).

Figure R-10. Aerodynamic effects of continuous and segmented 0.25 inch forward-facing quarter-round simulated ice shapes on the upper surface of an 18 inch chord NACA 23012m airfoil two-dimensional model (Re = 1.8×10^6, M=0.185) [R5].

R.4.2 Aerodynamic Considerations for Determining Critical Ice Shapes

Aerodynamic effects of ice accretions result primarily from the effects of the ice accretion on the surface's boundary-layer behavior. Ice accretions that occur in areas favorable to keeping the boundary layer attached to the aircraft or component surface will result in effects that are less aerodynamically adverse than ice accretions that occur in areas less favorable to attached boundary-layer conditions. Generally, ice shapes that accrete in areas of local airflow deceleration (positively increasing surface pressure) or result in conditions unfavorable to maintaining attached flow conditions as the airflow negotiates the ice surface will result in the most adverse effects.

For example, an ice accretion at the same chordwise location on different airfoils may result in different aerodynamic effects. Figure R-11 illustrates the surface pressure distributions for an uncontaminated NACA 23012 airfoil and an uncontaminated NLF 0414 airfoil at approximately the same lift. The NACA 23012 airfoil is forward-loaded, relative to lifting, and exhibits a severe pressure recovery (local airflow velocity deceleration to produce more positive pressures) downstream of the near-leading-edge suction pressure peak. The NLF 0414 airfoil's pressures and local velocities are much more constant with a pressure recovery occurring at approximately 0.7c, providing conditions conducive to maintaining a well-attached, laminar boundary layer over most of the airfoil's upper surface. Wind tunnel lift results (at low Reynolds numbers) from locating a ¼ inch simulated ice shape (quarter-round) at various chordwise locations on 18 inch models of each airfoil are shown in Figure R-12. Resultant maximum lift values are shown in Figure R-13. Although these aerodynamic characteristics are dependent upon the Reynolds number, the data illustrate the importance of the ice accretion location relative to the influence of the local flow conditions on the behavior of the boundary layer and airfoil aerodynamic performance.

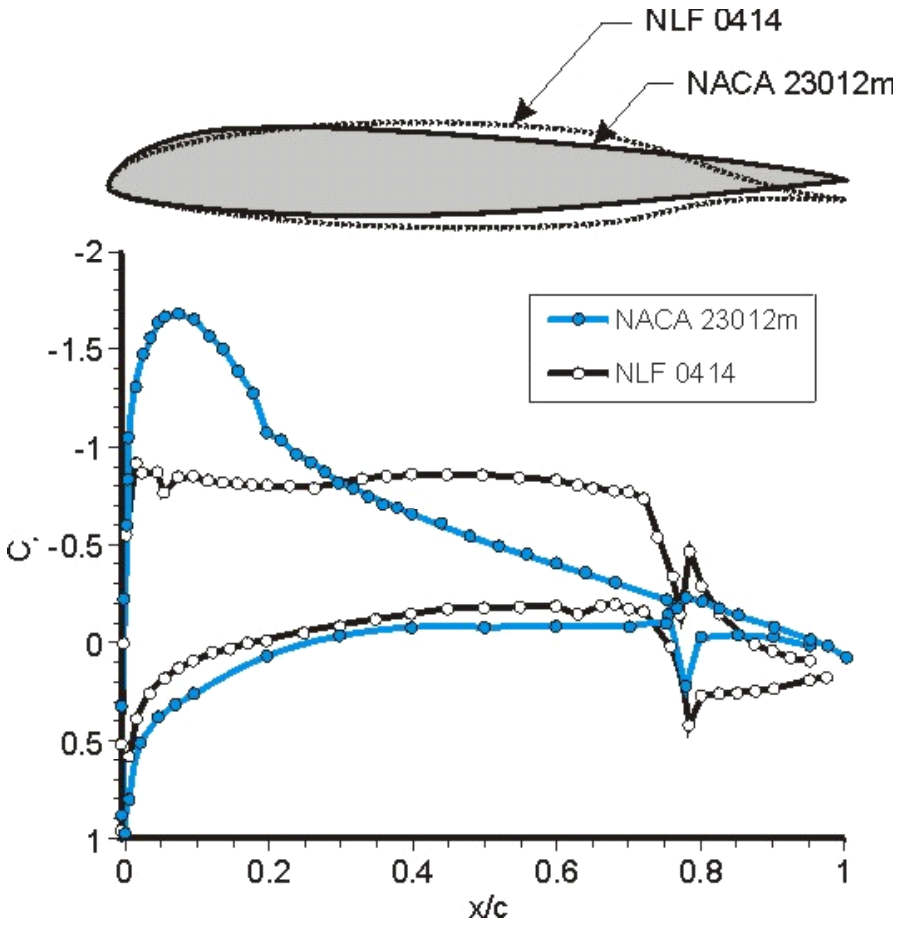

Figure R-11. Comparison of NACA 23012m and NLF 0414 clean airfoil model experimental pressure distributions ($C_l \sim 0.6$, Re = 1.8×10^6, M = 0.185) [R5].

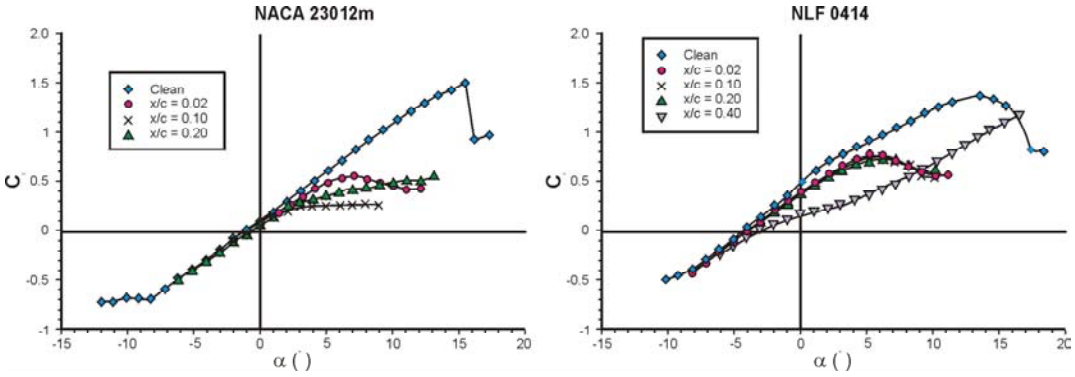

NACA 23012m **NLF 0414**

Figure R-12. Effect of an upper surface simulated quarter-round ice shape at various chordwise positions on lift for forward (NACA 23012m) and aft-loaded (NLF 0414) airfoils (k/c = 0.0139, Re = 1.8×10^6, M = 0.185) [R5].

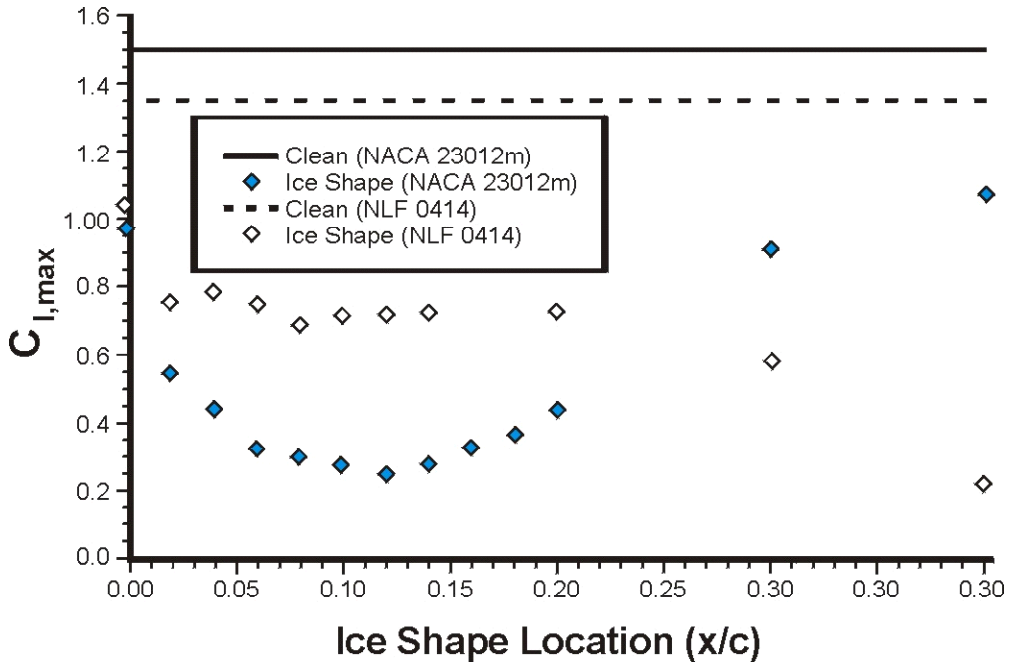

Figure R-13. Variation of $C_{l\,max}$ relative to clean airfoils, for NACA 23012m and NLF 0414 airfoils with a 0.25 inch forward-facing quarter round simulated ice shape located on the upper surface at various percent chord positions (Re = 1.8x10^6, M = 0.185) [R5].

The critical location, relative to maximum lift, for the simulated ice accretion on the NACA 23012 airfoil is approximately 0.125c; whereas for the NLF 0414 airfoil, the lowest maximum lift occurs at 0.40c (not shown). In both cases, the critical ice accretion location occurs near the area of the most severe pressure recovery (or, flow deceleration) for their respective stall angles-of-attack. (Note, pressure distributions shown in Figure R-11 are for normal operation attitudes.) Visual flow studies reveal that the separation bubble that forms downstream of the simulated ice shape on the NACA 23012 airfoil fails to reattach immediately downstream of the ice shape because of the rapid adverse pressure recovery gradient, resulting in a much longer separation bubble and a larger loss in maximum lift. Because of the less severe pressure recovery gradient on the NLF 0414 airfoil, the separation bubble is not as long, and the resultant maximum lift loss is not as severe as that of the NACA 23012 airfoil.

Relative to drag, the critical ice shape location for the forward-loaded NACA 23012 airfoil correlated with the area of highest local airflow velocity, not the area of most severe pressure recovery. This is shown in Figure R-14. However, the NACA 23012 ice shape location correlation did not apply to the results for the NLF 0414 airfoil, as shown also in Figure R-14. For the NLF 0414 airfoil ice shape drag increment, the critical ice shape location tended to suggest a sensitivity of the ice shape boundary-layer disturbance to the ability of the boundary layer to remain well attached during the pressure recovery at the aft part of the airfoil.

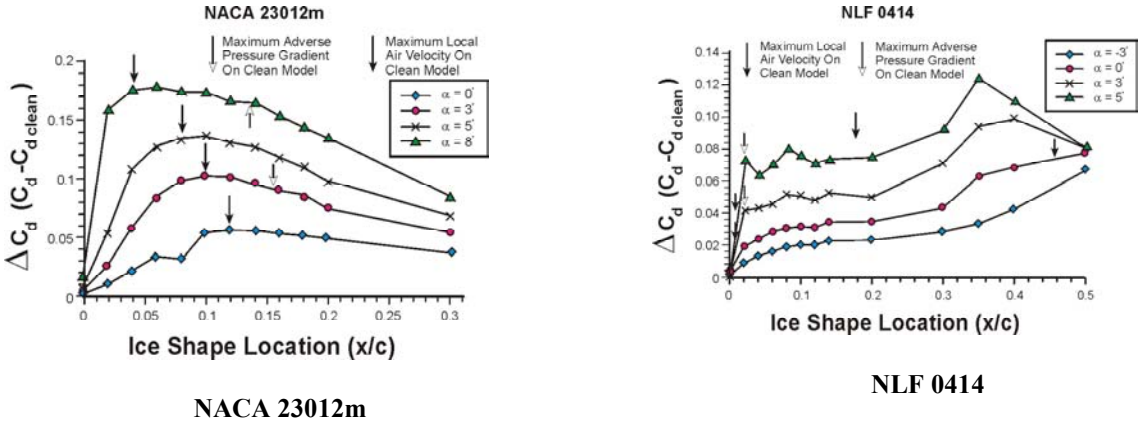

Figure R-14. Drag increase for NACA 23012m and NLF 0414 airfoils with a 0.25-inch forward-facing quarter-round simulated ice shape located on the upper surface at various percent chord positions (Re = 1.8×10^6, M = 0.185) [R5].

Another example that illustrates the importance of understanding the ice accretion shape's influence on the boundary-layer behavior when determining critical ice shapes is the comparison of rime and glaze ice shapes that have approximately the same mass. A rime ice leading edge ice shape that conforms with the profile of the aircraft surface may effectively improve the surface's camber, thereby improving local boundary-layer conditions and chord length. Conversely, the rime ice accretion may also thicken and weaken the boundary layer, causing the boundary layer to become turbulent or separated earlier than the contamination-free boundary layer. However, the resulting increased drag and reduced maximum lift will ordinarily be much less than that of a glaze ice shape of similar mass but with upper and lower horns that the airflow and boundary layer must negotiate. In fact, complete separation of the flow often occurs behind the horns. Also, the character of the boundary layer and its wake (turbulence intensity, tendency to remain turbulent, tendency to remain attached or to separate from the surface, and the periodicity of separation from the surface) may vary. These viscous flow effects will vary, depending on such considerations as:

- The Reynolds number.
- The size, shape, and surface roughness of the ice accretion.
- The relative size of the ice accretion protuberance and its surface roughness relative to the aircraft surface's characteristic size.
- The boundary-layer characteristics of the uncontaminated surface (that depend on the surface camber, thickness distribution, surface finish, and AOA).
- The location of the ice shape.

The boundary-layer effects resulting from the ice accretion typically manifest themselves in a relatively small loss of lift at operational aircraft angles-of-attack, but a significant loss in maximum lift and a significant reduction in the AOA at which maximum lift occurs. (See Figure R-8.) The loss in maximum lift may affect operational stall-speed margins, aircraft maneuverability margins to aircraft buffet, and stall warning margins unless operational airspeeds and the stall warning AOA are re-scheduled accordingly. Significant drag increase will occur at operational angles-of-attack, and the drag increase will accelerate with increasing AOA as the lower maximum lift AOA is approached. Rotary wings and propeller thrusting efficiency will be adversely affected. Surface pitching moments will be significantly changed toward a surface nose-down attitude as the

tendency of the boundary layer to remain healthy and attached and allow lift to be generated along the chord of the surface is changed by the ice accretion. These effects are evident in Figure R-8. Airplane stability and control characteristics, stall characteristics, and trim will be affected, as well as the performance of rotary wings and propellers.

The effects of Reynolds and Mach numbers on the performance of an airfoil with an ice accretion are shown in Figure R-15 for a 36-inch NACA 23012 airfoil with and without intercycle ice. For the clean airfoil, increasing the Reynolds number influences the behavior of the boundary layer, resulting in the boundary layer remaining attached to the airfoil at higher angles of attack. Also, for the uncontaminated airfoil, the improved boundary-layer behavior reduces drag at higher Reynolds numbers. However, for the airfoil with a simulated ice shape, the Reynolds number effects are much less significant. The effect of Mach number on airfoils with and without the simulated ice shape are illustrated in Figure R-15.

An evaluation to determine the surface or component critical ice shape for a specific flight safety aspect should reflect the above considerations. Evaluation of the aerodynamic effects of an ice accretion relative to an uncontaminated surface is significantly affected by the variation of the uncontaminated surface's aerodynamic characteristics with Reynolds and Mach numbers. For example, when the coefficients of lift and drag for a clean and a contaminated airfoil are compared, the differences between the uncontaminated and contaminated airfoils' coefficients are significantly affected by Reynolds and Mach numbers. Aerodynamic characteristics of contaminated surfaces do not always show large variation with Reynolds number, as shown in Figure R-15.

Downstream control surface pressure loading may be affected by critical ice shapes, resulting in reduced control surface authority, hinge moment and control force anomalies, and un-commanded control surface movement. The change in surface pressure loading and periodic separation of the surface airflow may also affect surface vibration and tendencies for surface flutter.

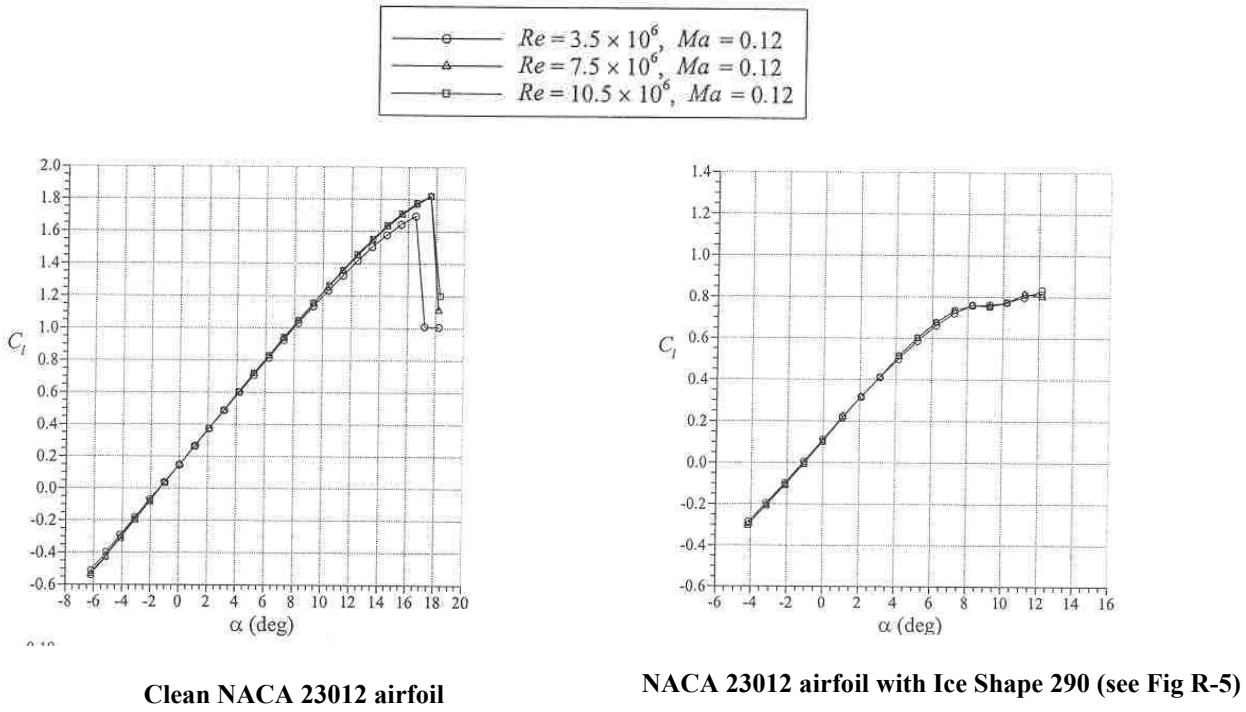

Clean NACA 23012 airfoil

NACA 23012 airfoil with Ice Shape 290 (see Fig R-5)

Figure R-15(a). Reynolds number effect on lift for a NACA 23012 airfoil with and without a simulated ice shape.

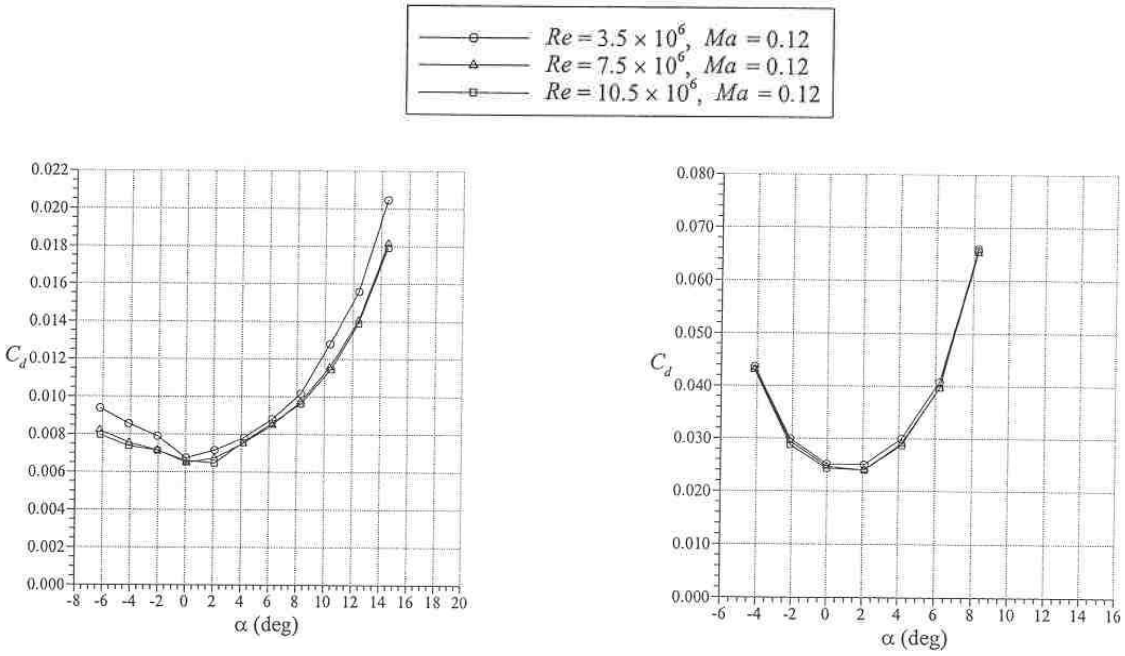

Clean NACA 23012 airfoil

NACA 23012 airfoil with Ice Shape 290 (see Fig R-5)

Figure R-15(b). Reynolds number effect on drag for a NACA 23012 airfoil with and without a simulated ice shape.

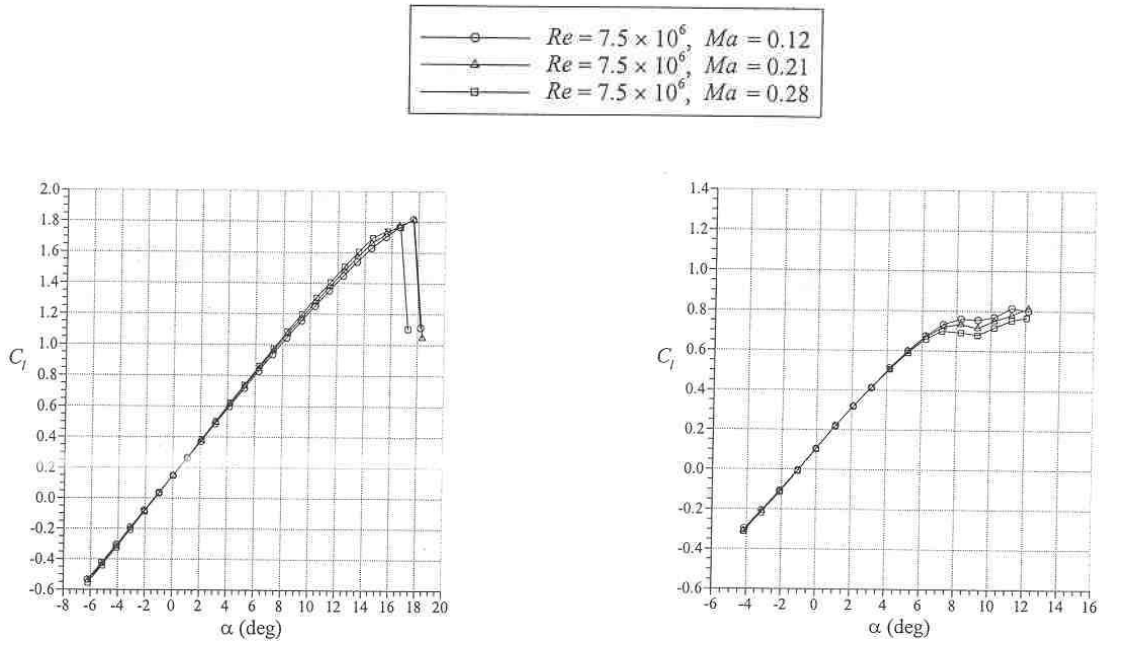

Clean NACA 23012 airfoil

NACA 23012 airfoil with Ice Shape 290 (see Fig R-5)

Figure R-15(c). Mach number effect on lift for a NACA 23012 airfoil with and without a simulate ice shape

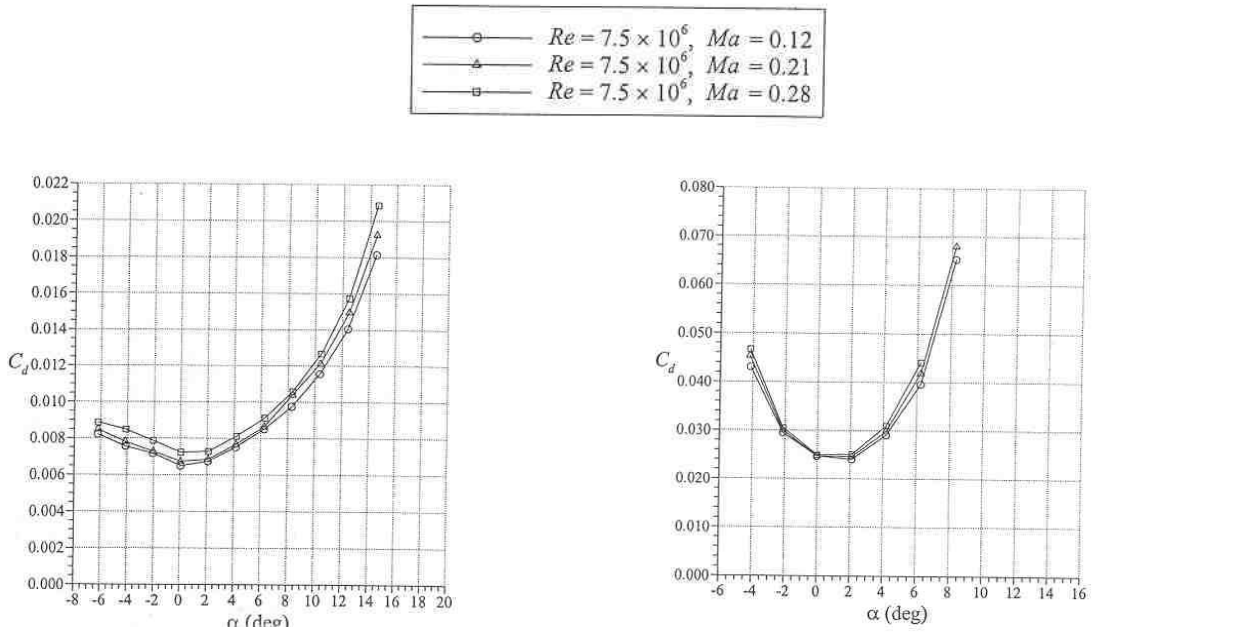

Clean NACA 23012 airfoil

NACA 23012 airfoil with Ice Shape 290 (see Fig R-5)

Figure R-15(d). Mach number effect on drag for a NACA 23012 airfoil with and without a simulate ice shape

Figure R-15. Reynolds and Mach numbers effects on lift and drag for a NACA 23012 airfoil with and without simulated Ice Shape 290 [R2].

The mass of the critical ice accretion on aerodynamically balanced control surfaces, such as elevator and aileron horns, may change the effectiveness of surface's aerodynamic balance and resulting hinge moments and control forces. Ice accretion mass on surfaces may also affect the control surface's tendency to vibrate or flutter.

Empirical aerodynamic data are typically used to determine the effects of critical ice accretions. Navier-Stokes CFD computer codes, if used carefully, may provide useful information.

The empirical aerodynamic data used should be applicable to the surface or component of interest since the aerodynamic effects of the ice accretion depend on the boundary layer's behavior over the surface and ice accretion. Empirical data are usually obtained for specific surfaces or components during flight, with simulated ice accretions or in natural icing conditions. Also, testing of scaled models with simulated ice accretions in dry air aerodynamic wind tunnels at appropriate Reynolds and Mach numbers may be used. However, these data should be cautiously used since replication of ice shapes at small scales is difficult and since data corrections beyond Reynolds and Mach numbers may be required to obtain results applicable to flight. An applicant that chooses to use scale models must substantiate that the performance information obtained with the scale models in a wind tunnel adequately duplicates the performance that would occur at full-scale.

Applicants may also have applicable empirical ice accretion effects data from similar or predecessor aircraft designs. Information available in the technical literature may be applicable, however the examination of the data is necessary to establish that the data is applicable to the aircraft design under consideration; also limited flight Reynolds number data are available. A survey of ice accretion effects, drawn from the open literature, and a discussion of critical ice shapes are provided in [R6]. Also, [R7] provides additional information relative to the aerodynamic effects of ice accretions. The ranking of ice shape features relative to their adverse aerodynamic effects provided in section R.6 – Correlation of Predicted (Simulated) and Natural Ice Shapes may be considered in determining the critical surface or component ice shape.

Appropriate CFD codes may also be used to determine the aerodynamic characteristics of critical ice accretions. Because the behavior of the airflow over the complex ice accretion shapes and roughness is highly affected by the air's viscosity, CFD codes predicated on solutions of the viscous flow Navier-Stokes equations, if carefully used, may provide useful information. Care is required to ensure that the gridding of the surface geometry and flow field is adequate and that the wake turbulence models used predicts the actual behavior of the boundary layer and its wake. The behavior of the boundary layer and its wake strongly influence the maximum lift and drag levels predicted by codes. Viscous flow CFD codes based on Reynolds-Averaged Navier-Stokes (RANS) equations (such as NSU2D and WIND), with sufficient attention given to gridding of the ice accretion shape and roughness and the flow field, provide good information at operational aircraft angles-of-attack. However, at attitudes where airflow separation occurs, such as when maximum lift is approached, the RANS codes may not robustly and accurately predict lift, drag, and pitching moments. This failure has been attributed various causes, including the inability of RANS codes to capture the vortex shedding physics of airflow separation that is of particular interest for complex ice shapes and roughness. This limitation of RANS codes is illustrated in Figure R-16 for an NLF 0414 airfoil with a simulated upper-surface ice shape horn. Good correlation with empirical data using a RANS code may be shown for an ice shape that exhibits insignificant vortex shedding at maximum lift, however the code may provide misleading information for other ice shapes that exhibit significant vortex shedding. Figure R-17 illustrates the periodic vortex shedding predicted by a Detached Eddy Simulation (DES) code for the above NLF airfoil configuration. (For additional information concerning DES codes, see [R8]). Also, because of the vortex shedding and its effects on the surface pressures, values of lift, drag, and pitching moment may become time-dependent; and, the code may fail to converge on a solution that provides acceptable averaged aerodynamic parameters.

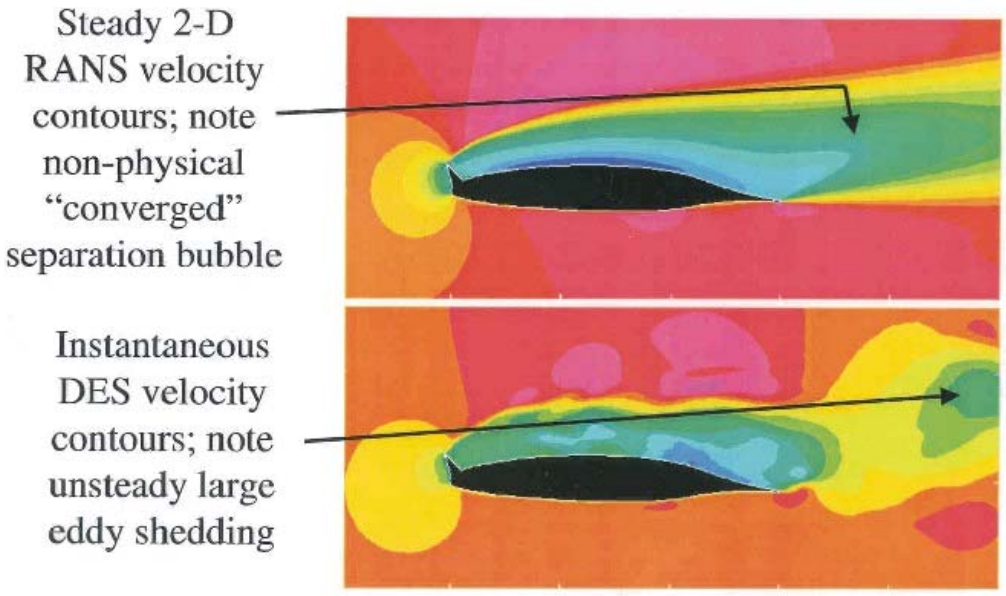

Figure R-16. Comparison of computed flow fields using Reynolds-Averaged Navier-Stokes (RANS) and Detached Eddy Simulation (DES) Navier-Stokes CFD codes (NLF 0414 airfoil at an AOA of 7° and a Reynolds number of 1.8×10^6 with a 0.034 k/c simulated ice shape horn) [R8].

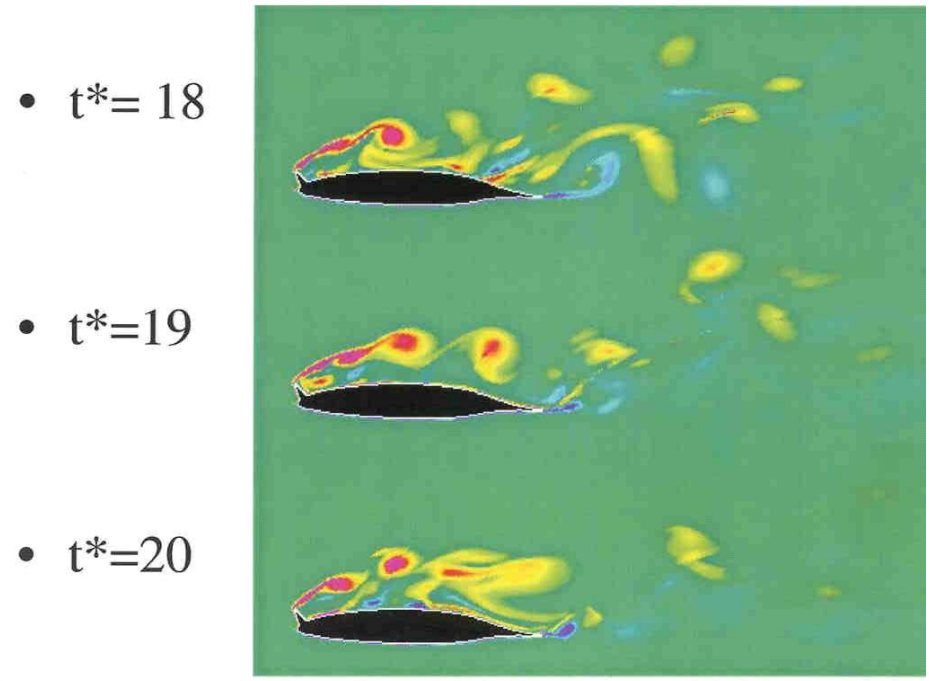

Figure R-17. Time-dependent vortex shedding (vorticity contours) from a NLF 0414 airfoil with a 0.034 k/c simulated ice shape horn calculated using a DES Navier-Stokes CFD code [R8].

Flow separation phenomena are three-dimensional, with lateral flow movement, especially for configurations which exhibit significant cross-flow velocity components, such as on swept, finite wings. The three-dimensional character of flow separation raises questions concerning the viability of two-dimensional Navier-Stokes flow solutions that exhibit significant boundary-layer separation. Figure R-18 illustrates the differences in upper surface flow separation and vortex shedding at the same time instant between two and three dimensional DES Navier-Stokes solutions for an 18-inch chord NACA 23012m model with a 0.25 inch quarter-round simulated ice shape located at ten percent from the leading edge. Direct Numerical Simulation (DNS) Navier-Stokes CFD codes that fully solve the Navier-Stokes equations or Large Eddy Simulation (LES) codes may be required to predict aerodynamic parameters confidently as maximum lift is approached. See [R9] for definitions and further discussions concerning RANS, LES, and DNS Navier-Stokes CFD codes. The cost of executing LES or DNS codes for complex geometry and the need to consider three-dimensional flow effects is very high, perhaps prohibiting their use when several candidate critical ice shapes are being investigated. Use of DES Navier-Stokes CFD codes (a hybrid between RANS and LES codes) may offer good, cost-effective information; however, these codes have not been fully evaluated relative to predicting flow behavior for surfaces with ice accretion shapes and roughness [R9].

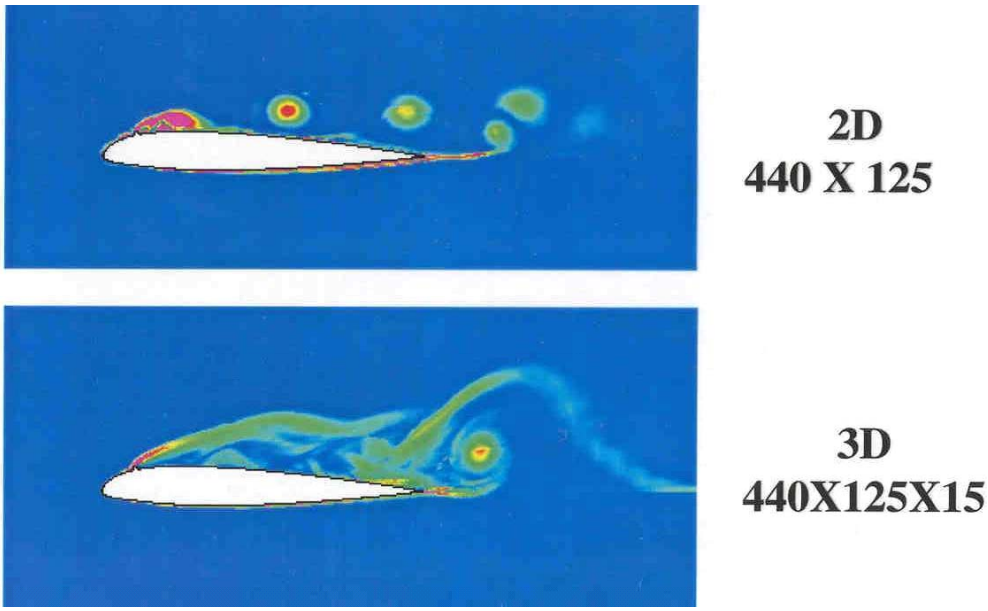

Figure R-18. Vorticity contours for two-dimensional (2D) and three-dimensional (3D) DES Navier-Stokes computational fluid dynamics code analysis of the flow field around a NACA 23012m airfoil with a k/c = 0.0139 forward-facing quarter-round simulated ice shape at the same time instant (Re = 1.8×10^6) [R8].

R.5 Methods for Determining (Predicting) Ice Shapes

R.5.1 Natural Icing Flight Tests

Ice shapes may be determined by flight tests in natural icing conditions. Unless means are available to accurately document the natural icing flight tests ice shapes for fabrication and installation of simulated ice shapes, testing for demonstrating that the aircraft can operate safely with the critical ice shapes should be performed with the natural ice accretions. Issues associate with demonstrating safe flight with natural ice shapes include availability of the icing conditions that produce the critical ice shapes and partial shedding, melting, and sublimation of the ice accretion during the flying qualities flight tests.

R.5.2 Use of Icing Tankers to Predict Unprotected Surfaces Ice Shapes

Icing tankers may be used to evaluate ice shapes for unprotected areas, particularly for complex, three-dimensional configuration areas that are difficult to predict by means of computer codes or other analytical methods. Also, use of icing tankers allows evaluation of ice shapes at full scale, and without concerns for ice accretion code or icing tunnel limitations. Generally, larger droplets of tanker icing cloud plumes are considered conservative for applications where a larger and more extensive ice shape is demonstrated to be conservative. The applicant should demonstrate that the icing tanker and associated instrumentation and icing plume are calibrated. Conformity with commonly accepted practices, as described in SAE ARP5904 [R10], should be considered when judging the acceptability of ice shapes derived from icing tanker flight tests. However, consistency of ice shapes produced by the different icing tankers for a given test article and similar artificial icing condition is unknown.

R.5.3 Use of Icing Wind Tunnels to Predict Unprotected Surfaces Ice Shapes

Icing wind tunnels are also used to predict ice shapes, especially for complex three-dimensional configurations. Additionally, icing wind tunnel ice shapes for simple, two-dimensional configurations are used to validate ice shapes derived from computer codes or other analytical methods.

Full-scale models of the aircraft component should be tested when feasible. Considerations should be given to immersion of the model in the calibrated test volume of the tunnel, tunnel blockage effects, and tunnel wall effects. The model's geometry should conform with type design drawings. When the full-scale model of the aircraft component is too large for the icing wind tunnel test section, hybrid or scaled models may be considered.

For airfoil testing, a hybrid scaling method may be used, in which the model replicates the full-scale airfoil or wing section and uses a trailing-edge flap to produce the desired flow conditions at the model's leading edge (see [R11], [R12], and [R13]). This method allows the use of a truncated model that produces less tunnel blockage and the desired use of operational ambient temperature, airspeed, liquid water content, drop size, and icing times. Limitations of the method include limited truncation of the model and the need to build several models if a large range of model angle-of-attack is of interest.

The basic Ruff method should be used for design of scaled icing wind tunnel models (see [R14] and [R15]). This method requires matching of the following:

- the modified icing cloud water droplet inertia parameter, K_0;
- the accumulation parameter, A_c;
- and the two energy-balance terms: the freezing fraction, n, and
- either the water-energy transfer parameter, φ, or the air-energy-transfer parameter, θ for icing wind tunnels with atmospheric total-pressure test sections.

For pressurized icing wind tunnels the Ruff method requires matching all of the similarity parameters. The scale tunnel velocity can be determined by matching either the Weber number (We) or the Reynolds number (Re). Good results have been obtained by determining the scaled freestream velocity by holding model-scale and full-scale Weber number (based on leading edge water film thickness) constant and holding the free-stream temperature the same (see [R16, R17]).

The droplet sizes involved should not be subject to splashing. Applicants should demonstrate that the icing tunnel and associated instrumentation are calibrated, that spray nozzles have been cleaned per the facility's procedures, that model-mounting effects are considered, and that the model is located within the calibrated test volume of the icing wind tunnel. (See [R18] for information concerning calibration of icing wind tunnels.) The icing wind tunnel model's configuration should conform to the aircraft's TC design. Ice protection operating pressures, temperatures, or current/voltage should take into account system tolerances.

Spray times may be adjusted to replicate the water catch (or the same scaling accumulation parameter A_c) for 14 CFR part 25, Appendix C cloud lengths. A common practice of adjusting spray time to obtain the same water catch when the target LWC cannot be achieved because of the icing wind tunnel's LWC capability is inappropriate, since only varying LWC results in different values of the scaling freezing fraction parameter, n_0. Scaling of obtainable test icing conditions to obtain ice shapes for target icing conditions should follow the above-recommended Ruff method that indicates that the scaling parameters of the target icing conditions be matched at the obtainable test icing conditions. Spray times up to 45 minutes need to be evaluated. Spray times may have to be adjusted for the time required for spray bar stabilization; the adjustment should be documented by the facility.

Figure R-19 correlates ice shapes obtained on a 53-cm reference NACA 0012 airfoil model with those obtained on a 27-cm half-scale model, with icing condition parameters of the half model scaled by holding the full model K_0, A_c, n, φ, and We_h constant. The data, obtained in the NASA Glenn Research Center Icing Research Tunnel, are shown for freezing fractions, n, ranging from 1.0 to 0.28, indicating the robustness of the scaling for freezing conditions ranging from rime ice to near-glaze ice.

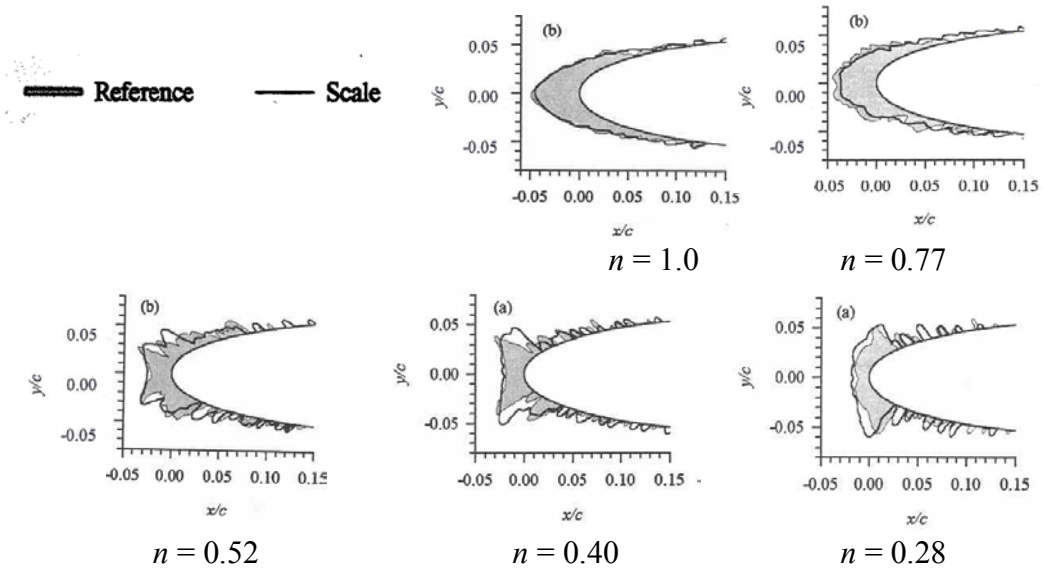

Figure R-19. Correlation of full-model (55 cm NACA 0012 airfoil) and half-model ice shapes by holding the full model K_0, A_c, n, φ, and We_h constant [R17].

Comparisons between icing wind tunnel and natural-ice simulated ice shapes are limited. However, visual comparisons of the detailed characteristics of three-dimensional wind tunnel (NASA-Glenn Research Center Icing Research Wind Tunnel [IRT]) and natural-ice simulated ice accretion on a 30º swept wing model, shown in Figure R-20, provide confidence in IRT ice shapes for the icing conditions evaluated (see [R19]). Conformance with SAE ARP5905 [R18] should be considered when judging the acceptability of icing wind tunnel ice shapes. Consistency of ice shapes produced by different icing wind tunnels for a given test article is being evaluated by the SAE AC-9C Subcommittee.

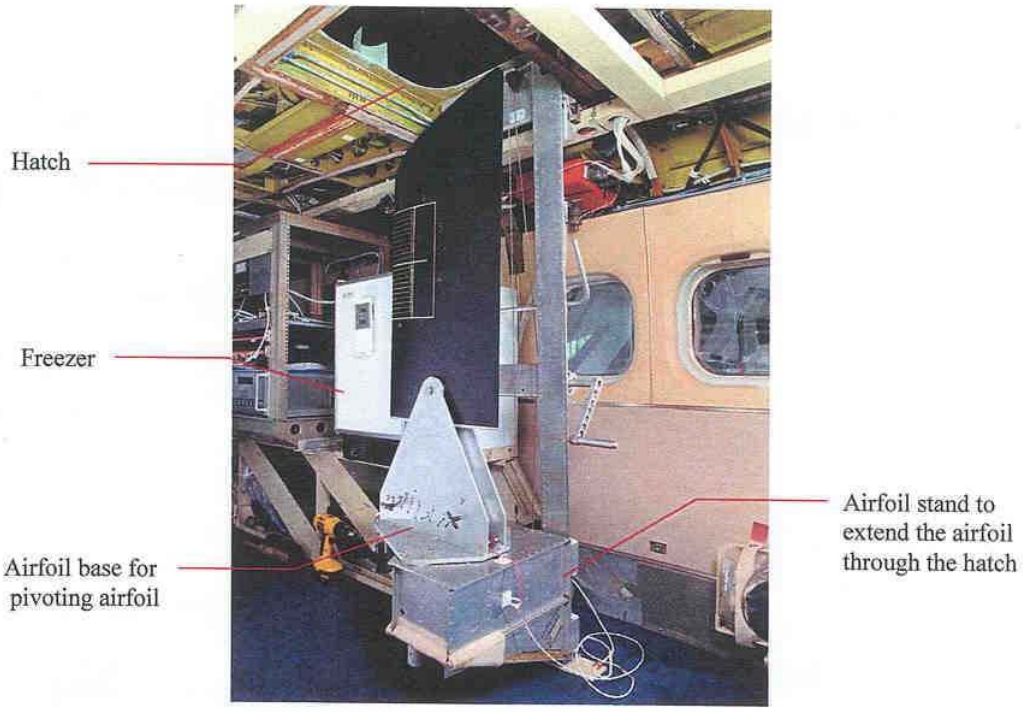

Figure R-20(a). View of the NACA 0012 swept wing model inside of the NASA Glenn Research Center Icing Research Aircraft (DHC-6 Twin Otter).

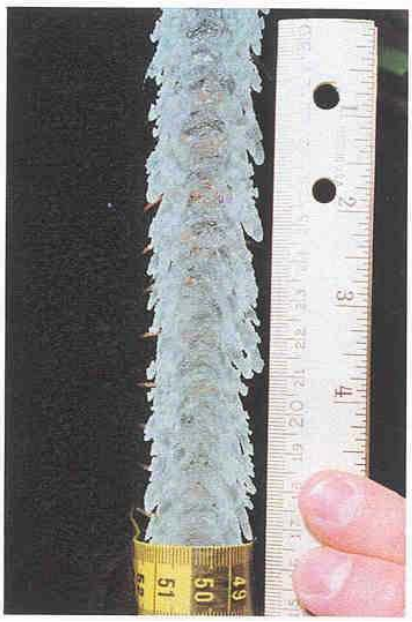

Figure R-20(b). Natural-ice ice accretion (scalloped) obtained with the NASA- GRC Twin Otter (Λ=30º, V=144 mph, T=21° F, LWC=0.45 g/m^3, MVD=13 µm, t=8 min.

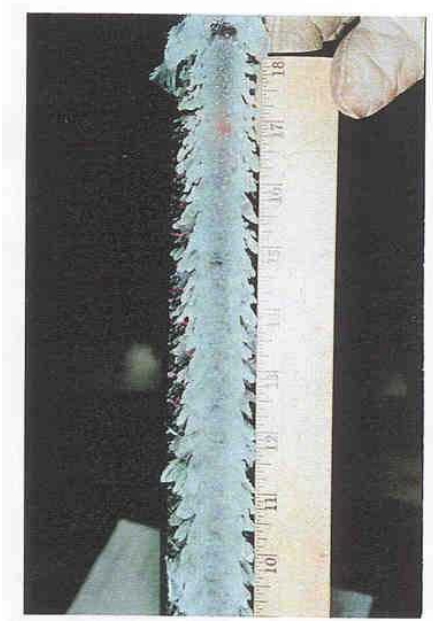

Figure R-20(c). Artificial-ice accretion (scalloped) obtained in the NASA-GRC IRT (Λ=30º, V=150 mph, T=25º F, LWC=0.5 g/m^3, MVD=20 μm, t=10 min.

Figure R-20. Comparison of natural and icing wind tunnel ice shapes [R19].

R.5.4 Droplet Impingement and Ice Accretion Computer Codes and Other Analytical Methods

Computer codes and analytical methods may be used to predict ice shapes. The predicted ice shape is the final result of calculations that define the flowfield, the drop trajectories, water loading, and the ice accretion physics. Many icing codes are currently available; they differ to varying degrees in their manner of modeling the ice accretion process. SAE ARP5903 [R20] provides information that describes several available droplet impingement and ice accretion codes.

When compared to icing wind tunnel ice shapes for two-dimensional airfoils, confidence in the ability of two-dimensional icing codes to accurately predict ice shapes is mixed. Reasons for this mixed confidence are illustrated in Figures R-21 through R-24, which show comparisons of ice shapes predicted by several icing codes with those obtained in two different icing wind tunnels. The data, derived from [R21], show that even at colder, rime ice conditions, where confidence in predicted ice shapes is thought to be highest, there are visually significant differences between the various predicted ice shapes and differences between the predicted and empirical ice shapes.

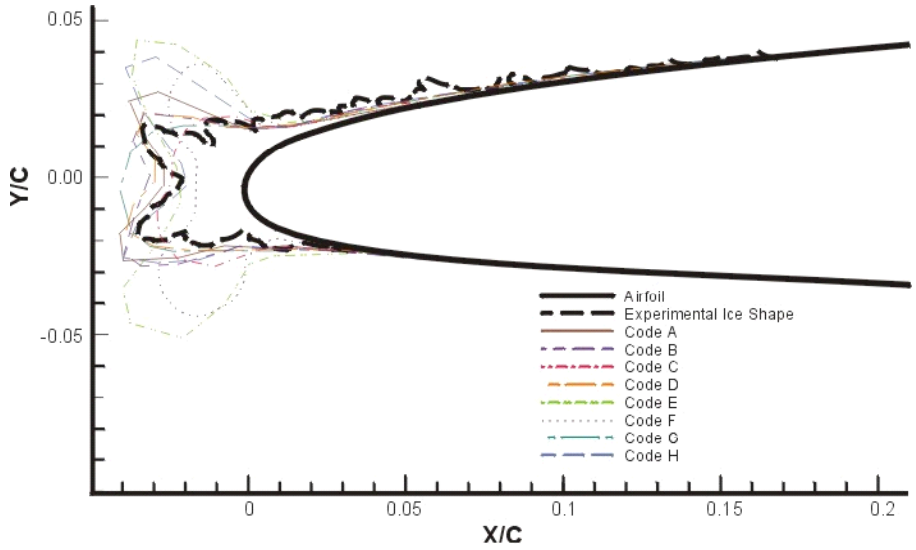

Figure R-21. Comparison of drop impingement and ice accretion code results with experimental ice accretion obtained in the NASA Icing Research Wind Tunnel (V = 135.8 kts, T_S = -15.8° C, LWC = 1.16 g/m^3, MVD = 50.0 µm, icing duration = 517.1 s, GLC305-836-23 airfoil model chord = 0.9144 m) [R21].

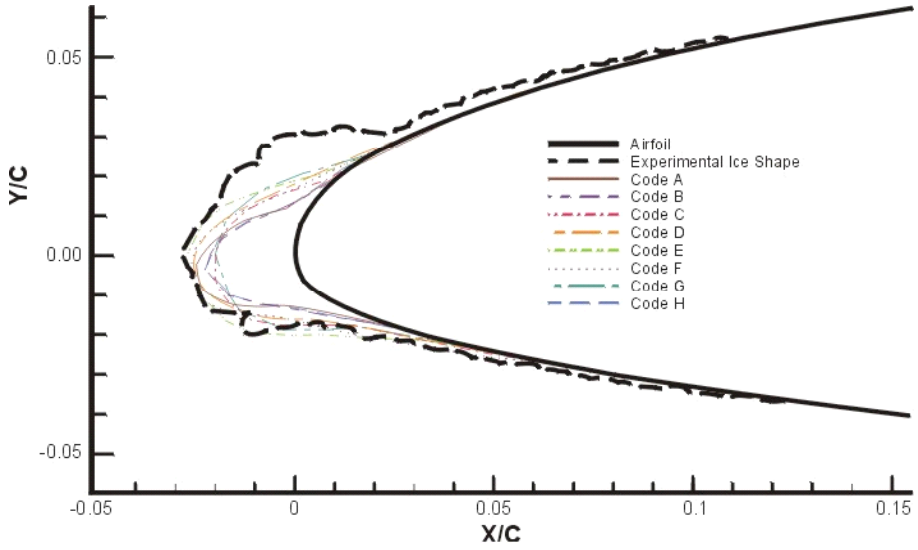

Figure R-22. Comparison of drop impingement and ice accretion code results with experimental ice accretion obtained in the NASA Icing Research Wind Tunnel (V = 179.8 kts, T_S = -15.6° C, LWC = 0.33 g/m^3, MVD = 20.0 µm, icing duration = 1224.0 s, NLF0414-611 airfoil model chord = 0.9144 m). [R21]

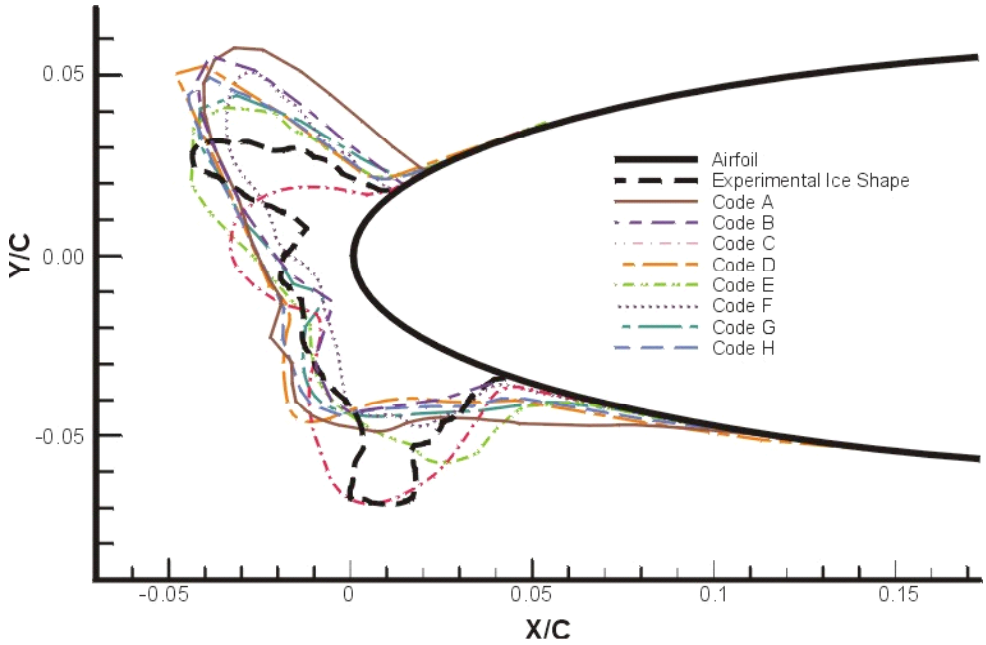

Figure R-23 **Comparison of drop impingement and ice accretion code results with experimental ice accretion obtained in the Boeing Research Aerodynamic and Icing Wind Tunnel (V = 130.2 kts, T_S = -7.2 ° C, LWC = 1.0 g/m^3, MVD = 24.8 µm, icing duration = 1200.0 s, airfoil model chord = 0.914 m) [R21].**

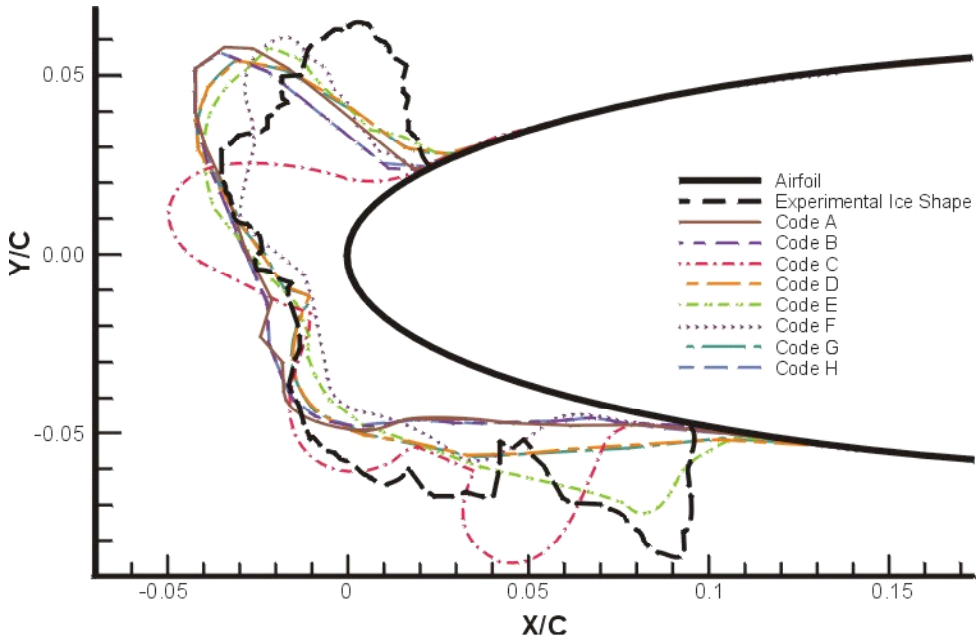

Figure R-24. **Comparison of drop impingement and ice accretion code results with experimental ice accretion obtained in the Boeing Research Aerodynamic and Icing Wind Tunnel (V = 130.2 kts, TS = -7.2 ° C, LWC = 1.0 g/m3, MVD = 38.8 µm, icing duration = 1200.0 s, airfoil model chord = 0.914 m) [R21].**

Ice accretion codes with three-dimensional flow field and droplet trajectory capability, coupled to a two-dimensional ice accretion calculation, have been or are being developed to predict three-dimensional ice shapes. The experimental ice shape data available at this time for validating these pseudo three-dimensional ice accretion codes is limited. Therefore, confidence in these ice accretion codes is yet to be established. Furthermore, none of the codes incorporates a capability to predict the experimentally-observed periodic "scalloped" or "lobster tail" ice shapes that develop from ice feathers on swept wings.

Many factors contribute to the acceptability of icing codes. These include selecting an icing code that has been developed to address the application of interest, the demonstrated validity of the code for the application, administration of the code software (including software configuration control and appropriate documentation), and the skill of the user. Useful information relative to judging the acceptability of icing codes is provided in SAE ARP5903 [R20].

As discussed above, confidence in the accuracy of ice accretion codes is mixed; therefore, ice accretion code ice shapes should be evaluated conservatively for their ability to ensure safe flight in the applicable icing conditions or as limited by the aircraft's flight envelope. Conservative results from icing code ice shapes will cause a more adverse handling quality effect or/and greater performance penalty, as compared with results from an applicable reference ice shape. (See R.4 – Critical Ice Shapes.) The applicant should provide substantiation that ice shapes selected from icing codes and analytical methods are conservative, including evaluating the effects on aircraft handling, performance, structural vibration, shedding, and airflow disturbance affecting downstream components and systems. Such substantiation may be difficult to produce without providing an applicable validated ice shape for reference, resulting in the need to validate the selected computed ice shape with an empirically determined ice shape, preferably from flight in atmospheric icing conditions.

R.5.5 Prediction of Landing Gear and Strut Ice Shapes

For fixed gear aircraft and for gear-down dispatch deviation operations of aircraft with retractable landing gear, ice shapes for the landing gear components may be estimated conservatively by analysis or artificial (tanker) icing tests. Strut ice accretion shapes may be estimated by any of the icing simulation methods.

R.5.6 Prediction of Protected Surfaces Ice Shapes

Prediction of protected surfaces ice shapes, such as intercycle ice of deicers, may be accomplished at full scale in natural icing or artificial icing conditions (tankers and icing wind tunnels). See sections R.5.1, R.5.2, and R.5.2 for additional guidance information. Testing of full-scale protected surfaces in the icing wind tunnel using the hybrid-model method may be accomplished provided the ice protection system conforms with the type design of the system. Time histories of pressure or temperature increases during activation should be compared to the actual aircraft. In the case of pneumatic deicing boots, this may require adding air volume in the system test set-up. The test matrix should include longer times in Continuous Maximum conditions to evaluate the stability and cyclic nature of intercycle and residual ice. Certain unique design features, such as stall strips mounted on deicing boots, may not readily shed ice.

Confidence in the use of scaled models with scaled ice protection systems to predict intercycle ice, runback ice, and other ice protection design parameters has not been established.

R.6 Correlation of Predicted (Simulated) and Natural Ice Shapes

To verify the safe operation of the aircraft, the flying qualities of the aircraft with simulated ice shapes should be compared to those of the aircraft with natural ice shapes. Comparison of the simulated ice testing with that in natural icing may be difficult and require engineering judgment. There may be a limited amount of quantitative flight characteristic data available for comparing the natural and simulated ice shape test results. Natural icing conditions are variable, especially during lengthy exposures or during series of brief exposures required to accrete the desired ice thickness. Close examination of the resulting accreted ice shapes on the

flight test aircraft is often impractical, and the icing conditions that were used to determine the simulated ice shapes may not match the natural icing conditions encountered. The simulated ice shapes also may reflect a composite of critical ice shape considerations (such as horn length, location, angle, and mass). Natural icing tests, however, are required to provide overall checks of the aircraft's safe operation in icing conditions, IPS analyses, simulated ice shape analyses, and unforeseen icing anomalies. Aircraft performance and handling qualities demonstrated during natural icing flight tests should be equivalent or less affected by ice accretion than those demonstrated with the simulated ice shapes.

Lists of ice shape and water catch evaluation parameters, ranked relative to adverse airplane effects, which may be used to compare simulated and natural ice shapes, are provided in Tables R-1 and R-2, respectively. These lists are derived from SAE ARP5903 [R20].

Table R-1. Ranking of Ice Shape Evaluation Parameters

Rank	Parameter	Units	Conservatism Criteria.
1	Upper (suction surface) horn height	-	Equal or greater horn peak thickness (height)
2	Upper Horn Angle	Degrees	Criticality of location (at upper peak thickness)
3	Lower (pressure surface) height	-	Equal or greater horn peak thickness (height)
4	Lower Horn Angle	Degrees	Criticality of location (at lower max. thickness)
5	Total ice cross-sectional area	-	Equal or greater area
6	Leading edge minimum thickness	-	Equal or smaller thickness
7	Upper accretion limit	% x/c*	Equal or greater x/c
8	Lower accretion limit	% x/c*	Equal or greater x/c

(Note that the first four parameters presuppose that icing horns exist, which is not always the case.)

* Percent of local component chord

Table R-2. Ranking of Water Catch Evaluation Parameters

Rank	Parameter	Units	Conservatism Criteria.
1	Upper impingement limit (suction surface)	% x/c*	Equal or greater x/c
2	Lower impingement limit (pressure surface)	% x/c*	Equal or greater x/c
3	Total water catch efficiency, E	-	Equal or greater magnitude
4	Maximum local water catch magnitude	-	Equal or greater efficiency, βmax
5	Water catch efficiency (Beta) curve	-	Equal or more adverse β distribution

* Percent of local component chord

Reasons why ice shapes produced by various icing wind tunnels, computer codes, and other analytical methods vary include:

- The uniformity and qualities of the tunnel's flow and icing plume
- Other tunnel testing considerations

Reasons why ice shapes produced by various ice accretion computer codes, and other analytical methods, vary include:

- Differing algorithms and assumptions used in the computer codes and analytical methods
- The use of various computer code versions and inputs

- The use of empirical ice shapes from different sources to "tune" computer codes and other analytical methods (to account for unknown icing physics and other effects)

Once satisfactory correlation has been established between icing wind tunnel, computer codes, and analytical method with the validation database, configuration control for these simulation ice shape methods should be established to maintain confidence in the simulated ice shapes provided by the methods. Engineering judgment is required to understand the limitations of the established correlation. For example, a correlation may continue to exist for changes in a single-element airfoil's thickness, thickness distribution, and camber. But, a correlation established for a single element airfoil should be questioned if applied to a multi-element airfoil. Also, a correlation established for two-dimensional airfoils may not be used for three-dimensional configurations.

R.7 References

R1. **"A Study of Inter-cycle, Residual, and Preactivation Ice,"** Riley, J. T., et al., AIAA-2001-0089, 39th AIAA Aerospace Sciences Meeting and Exhibit, January 8-11, 2001, Reno, Nevada.

R2. **Effect of Intercycle Ice Accretions on Airfoil Performance,"** Broeren, A.Pl, Addy, H.E. Jr., and Bragg, M.B., AIAA-2002-0240.

R3. **NPA 25F-219; Flight Characteristics in Icing Conditions**, Joint Aviation Authorities Letter JAA/SEC/3-9-2, dated 23 April 1993.

R4. **Empennage Deicing System Deletion**, Malone, Frank, Boeing Airliner, May-June 1962.

R5. **"Effects of Large-Droplet Ice Accretion on Airfoil and Wing Aerodynamics and Control,"** Bragg, Michael B. and Loth, Eric, Aeronautical and Astronautical Engineering, University of Illinois at Urbana-Champaign, August 16, 1999.

R6. "Report of the 12A Working Group on Determination of Critical Ice Shapes for the Certification of Aircraft," FAA Report Number DOT/FAA/AR-00/37, Office of Aviation Research, Washington, D.C. 20591.

R7. "Effects of Ice Accretions on Aircraft Aerodynamics," Lynch, F.T. and Khodasdoust, A., Progress In Aerospace Sciences, January, 2002.

R8. **"DES For Airfoils With Upper-Surface Ice Shapes,"** Pan, J. and Loth, E., Department of Aeronautical and Astronautical Engineering, University of Illinois at Urbana-Champaign, September, 2001.

R9. "Detached Eddy Simulations of An Iced-Airfoil," S. Kumar and E. Loth, AIAA Paper AIAA 2001-0678.

R10. **"Airborne Icing Tankers,"** SAE ARP5904.

R11. von Glahn, U.H., "Use of Truncated Flapped Airfoils for Impingement and Icing Tests of Full-Scale Leading-Edge Sections," NACA RM E56E11, July 1956.

R12. Saeed, F., Selig, M.S., and Bragg, M.B., "Design of Subsonic Airfoils with Full-Scale Leading Edges for Ice Accretion Testing," AIAA-96-0635, January 1996 and J. Aircraft, vol.34, no. 1, January-February 1997, pp 94-100.

R13. Saeed, F., Selig, M.S., and Bragg, M.B., "Experimental Validation of the Hybrid Airfoil Design Procedure for Full-Scale Ice Accretion Simulation," AIAA-98-0199, January 1998.

R14. Ruff, G.A., "Analysis and Verification of the Icing Scaling Equation," AECD-TR-85-30, Vol 1 (Rev), March 1986.

R15. Anderson, D.N., "Manual of Scaling Methods," Ohio Aerospace Institute (to be published).

R16. Anderson, D.N., "Effect of Velocity in Icing Scaling Tests," AIAA-2000-0236, January 2000.

R17. Kind, R.J., "Assessment of Importance of Water-Film Parameters for Scaling of Glaze Icing," AIAA-2001-0835, January 2001.

R18. **"Calibration and Acceptance of Icing Wind Tunnels,"** SAE ARP5905.

R19. **"Ice Accretion Formations on a NACA 0012 Swept Wing Tip in Natural Icing Conditions,"** Vargas, M., Giriunas, J.A., and Ratvasky, T.P., AIAA-2002-0244.

R20. **"Ice Accretion and Droplet Impingement Codes,"** SAE ARP5903.

R21. "**Ice Accretion Simulation Evaluation Test**," NATO RTO Technical Report TR-038, November 2001.

APPENDIX S. ICE-CONTAMINATED HORIZONTAL STABILIZER (TAILPLANE) STALL.

S.1 Ice-contaminated Horizontal Stabilizer (Tailplane) Stall.

As discussed in Section 6.1 – Applicable Regulations, safe flight of airplanes in icing conditions requires compliance with 14 CFR parts 23 and 25 § .143. Numerous accidents have resulted from stalling of an ice-contaminated horizontal tail. This phenomenon is commonly called ice-contaminated tailplane stall (ICTS). Typically, the accidents occurred during the approach phase of flight with the wing flaps extended.

Typically, the horizontal tailplane generates down-lift to balance the pitching moment created between the wing lift and the center of gravity, as shown in Figure S-1. The amount of down-lift required by the horizontal tail to balance the pitching moments varies with the airplane flap configuration and flight condition (airspeed/angle-of-attack and thrust). When the flaps are extended, the wing center of lift moves further aft of the center of gravity, causing an increased nose-down pitching moment (Figure S-1). Additionally, the extended wing flap increases the wing camber, resulting in an increased wing lift for a given angle-of-attack and an increased circulation of chord-wise airflow around the wing. The flight condition also has an effect on the pitching moment. Decreasing airspeed/increasing aircraft angle-of-attack requires an increase in tail down-lift. Increasing the thrust may also affect the pitching moment depending on the position of the thrust line with respect to the center of gravity. All of these effects necessitate an increase in the tail down-lift in order to balance the airplane in the pitch axis.

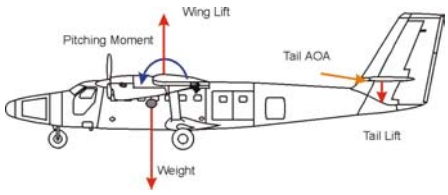

Cruise Configuration

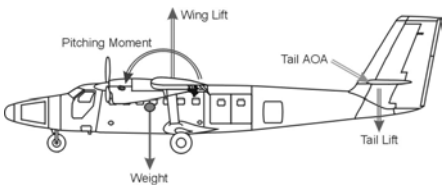

Trailing edge flaps extended

Figure S-1. Airplane forces and pitching moments.

This balancing is accomplished by increasing the angle-of-attack at the tailplane, and/or deflecting the elevator position to modulate the tail down-lift. The angle-of-attack at the tailplane is strongly affected by the wing trailing edge flap position. With flaps extended, there is a significant increase in downwash, which increases the angle-of-attack at the tailplane. This increase in the angle-of-attack at the tailplane effectively increases the tail down-lift. The angle-of-attack at the tailplane may be adjusted further if the airplane has a trimmable horizontal stabilizer. Otherwise, the elevator position can be deflected to provide the down-lift required for balance.

The tail down-lift requirements remain the same when ice accretes to the horizontal tail. However, the capability of the horizontal tail to produce the down-lift is degraded. Figure S-2 shows that a small amount of roughness, such as that resulting from a thin accretion of ice on the leading edge of a horizontal stabilizer may cause the horizontal tail to stall at a lower angle-of-attack (relative to the uncontaminated tail). Flight testing with 'sandpaper' ice has been shown to be more severe than classical ice shapes on some aircraft and needs to be evaluated in the certification program. However wind tunnel testing of a 36-inch NACA 23012 airfoil at a Reynolds number of 7.5×10^6, as shown in Figure R-8 of Appendix R, indicates that intercycle ice surface roughness may be more adverse than sandpaper ice.

In ICTS, the flow separation of interest typically starts at the leading edge and progresses aft over the lower surface of the tailplane to some line where the flow reattaches. As the angle-of-attack increases, the line of reattachment moves further aft. If the flow separation moves aft to the elevator control surface, a significant hinge moment in the trailing edge down direction will occur because of redistributed pressures on the elevator.

If this occurs with an unboosted elevator control system, the increased hinge moment may snatch the control column forward from the pilot and require significant pilot strength to counteract. The elevator will automatically deflect trailing edge down until the hinge moment reaches zero as the pressures on the upper and lower surface of the elevator surface equalizes (unless controlled by the pilot), further reducing the pitch controllability and stability.

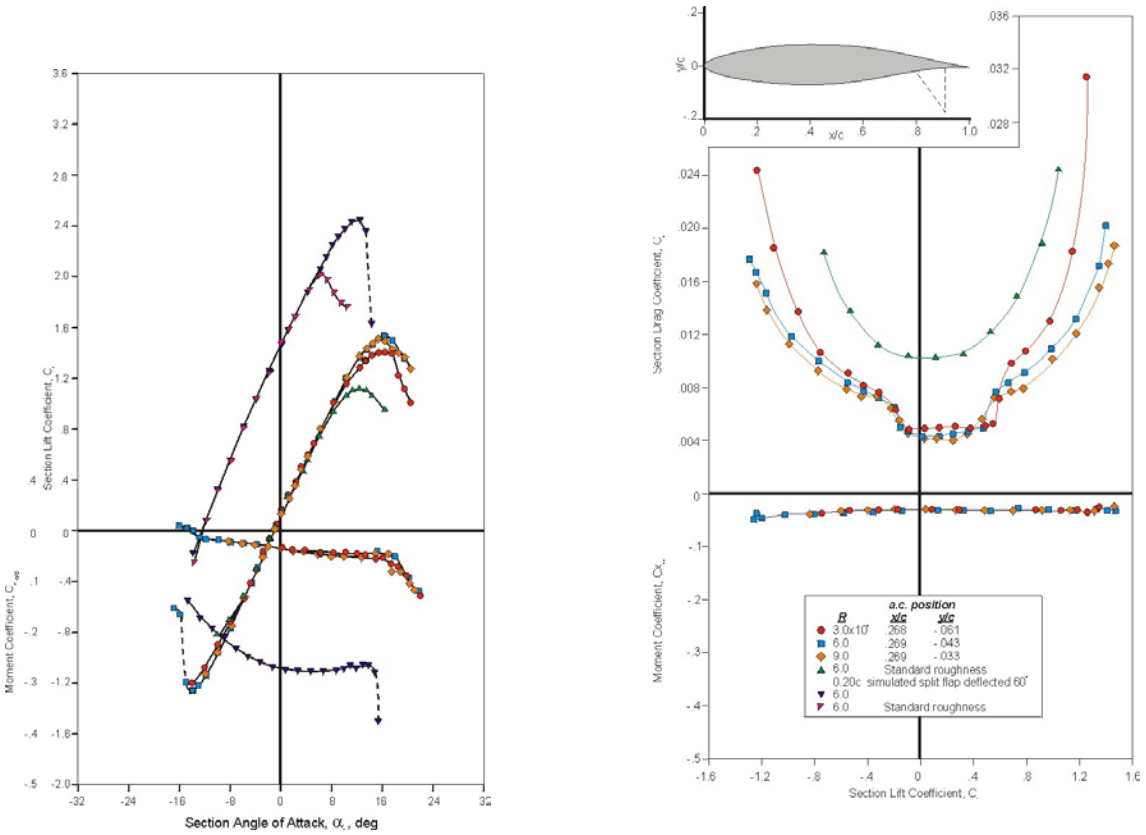

Figure S-2. Standard roughness (0.011 inch carborundum grains uniformly distributed at a density of five to ten percent of the area extending from the airfoil's leading edge to 0.08c of the 24 inch model) aerodynamic effects for a NACA 652-215 airfoil [S1].

ICTS occurs when the iced stall angle-of-attack is exceeded, and that angle-of-attack may vary with different ice shapes. The primary driver for increasing the angle-of-attack at the tail is the wing trailing-edge flap as discussed above. However, other factors that can lead to exceeding the iced tail stall angle are nose-down pitch motion (to capture a glide slope), reduced airplane angle-of-attack to increase airspeed, wind gusts, and changes in engine power. Additionally, the airflow about the tailplane may be aggravated by local flow interactions emanating from the juncture of the horizontal and vertical stabilizers for cruciform and T-tail designs during high sideslip maneuvers.

Accidents caused by ICTS have occurred when the airplanes were on approach and at low altitude. Flight operations near the ground do not allow much time for the crew to distinguish between a wing stall and tail stall, and then to perform the proper piloting technique to recover control of the airplane. If ICTS occurs, the pilot technique to recover control is to reduce the angle-of-attack at the tailplane by raising the flaps and pulling back on the control column to raise the nose.

Aerodynamic effects of ice-contaminated horizontal stabilizers should be considered for all airplanes, including those with tab driven controls and those with powered controls. An evaluation should be made to determine if this unsafe flight condition is likely to occur. Airplanes susceptible to this phenomenon are those having

horizontal stabilizers that operate uncontaminated with little or no margins to stall. Acceptable flight test procedures for determining the susceptibility of an airplane to this phenomenon are presented in ACs 23.143-1 and 25-7A. Additional guidance information is provided in AC 23.1419-2B and AC 25-1419-1.

S.2 References

S1. **"Theory of Wing Sections,"** Abbot, Ira H. and Von Doenhoff, Albert E., Dover Publications, Inc., 180 Varick Street, New York, N.Y., 10014, 1959, p. 626-627.

APPENDIX T. ARTIFICIAL ICING FLIGHT TESTS: AIRBORNE ICING TANKERS AND SPRAY RIG TESTS.

T.1 Airborne Icing Tanker Tests

Artificial icing conditions developed by icing tankers have been used successfully to check analyses required for showing regulatory compliance, including droplet impingement information, to check or develop simulated ice shapes, measurement of heat transfer coefficients, and ice shedding from selected aircraft components. Information obtained during icing tanker tests may also be used to check small-scale tunnel test results and to extend natural icing tests to icing conditions within Appendix C not obtained during natural icing tests. The results must be shown to be both accurate and conservative. Icing tankers, especially those that have hydraulically-aspirated nozzles, may not be able to completely reproduce Appendix C icing conditions. See SAE ARP5904 [T1] for additional information.

T.2 Spray Rig Tests

Certain areas or components of airplane icing systems can be tested by installing spray rigs on the airplane that deploy water droplets which impinge on the surfaces of interest during flight. Some of the limitations applicable to tanker tests also apply to spray rig tests. Test rigs of this nature are expensive to develop and to install on test aircraft. An advantage of this type of testing is the ability to control the distance between the spray section and the test surface, but the droplet transit time must be long enough for the droplets to reach a supercooled state. The major disadvantage of this method is the possible disruption to the flow field around the test surface due to the presence of the rig itself. This feature may produce unrealistic impingement characteristics that are difficult to evaluate. Studies, such as wind tunnel tests, may be required to ensure that the test surface icing environment is not contaminated by the disturbance of the test rig. The size and weight restrictions of the spray rig structure also limit the area that can be subjected to the spray. Because of the limitations of this test method, it is not generally considered adequate for showing full compliance with the regulations; however, this does not eliminate its use as a development tool or for testing relatively small areas for icing.

T.3 References

T1. “Airborne Icing Tankers,” SAE ARP5904.

APPENDIX U. ICING WIND TUNNEL TESTS.

U.1 Icing Wind Tunnel Tests

Several types of wind tunnels, including closed and open loop, refrigerated and atmospherically cooled, have the ability to simulate icing conditions. These facilities have the ability to produce controlled, steady-state plumes of supercooled water drops throughout a range of temperatures, LWC, droplet size, and airspeeds to simulate a variety of operational conditions. They allow direct access to examine ice accretions and to measure IPS performance quite accurately. Instrumentation for measuring the icing cloud is generally more extensive and accurate than flight test instrumentation; also direct control of the icing conditions is provided by the icing wind tunnel. The icing tunnel should be in calibration, following the practices described in SAE ARP5905 [U1]. Conformance with SAE ARP5905 should be considered when judging the acceptability of information obtained in icing wind tunnels. The disadvantages of ice tunnel tests are their limited size and, typically, their inability to simulate altitude effects and the variability of icing conditions normally experienced during natural icing conditions.

Most tunnels are small, compared with the sizes of desired test articles. Obtaining accurate aerodynamic and thermodynamic similarity for models of large components, with tunnel blockage on the order of 10 percent or more, may be difficult. Wind tunnel flow characteristics, icing plume uniformity, wall effects, model effects, model support, and model scaling issues should be addressed. A dimensional analysis of the aerodynamic and thermodynamic parameters which describe the full-scale system should be undertaken prior to model tests to ensure similarity between the full-scale and model-scale systems, including consideration of Reynolds and Weber numbers. See Appendix I – Droplet Impingement Limits and Water Catch and Appendix R, Section R.5.3 – Use of Icing Wind Tunnels to Predict Unprotected Surfaces Ice Shapes for further discussion concerning the use of scaled models for drop impingement and ice shape investigations. Full-scale values may be determined from natural icing flight tests, dry air flight tests, spray rig tests, tanker tests, or a combination of these tests.

Test conditions and models should be designed to ensure that Reynolds Number and other scaling parameters are maintained as closely as possible to the full-scale value. Test models should be mounted to simulate the flight attitude associated with the most critical condition. If flaps or other devices are used to produce the proper flow field conditions, instrumentation should be provided to show that test and design parameters are in agreement. In an ice tunnel test of an evaporative system, all of the impinging water should evaporate.

Liquid systems tested in an icing tunnel should preclude ice formation on the protection surfaces for the designed period of protection, with flow of temperature depressant fluids within the design value.

U.2 References

U1. “Calibration and Acceptance of Icing Wind Tunnels,” SAE ARP5905.

APPENDIX V. AIRCRAFT FROST AND CLEAR ICE CONSIDERATIONS.

Frost is a form of ice and can adversely affect aircraft handling qualities and performance. Frost will accrete on aircraft surfaces if the surface temperature is below the ambient dew point (resulting in condensation of ambient moisture) and when the surface temperature is below the freezing point. Frost commonly accretes on aircraft parked outside overnight, even when ambient temperatures may be above freezing since the aircraft surfaces may radiate heat to the atmosphere and become cooler than the ambient air. Also the aircraft's surface temperature rise may lag that of the ambient air due to the thermal mass of the aircraft. Aircraft surface exposed to sunlight will have a temperature rise because of radiant heating and may not accrete frost, whereas surfaces protected from the sunlight may have frost during subfreezing ambient temperatures. Frost may occur in different crystalline formations, ranging from a thin, relatively smooth coating to a thick, granular, rough coating, such as hoarfrost. Thick hoarfrost may obliterate painted marking on fuselages.

Fuel at sub-freezing temperatures may result in the formation of frost or clear ice on aircraft surfaces. Sub-freezing fuel stored in in-spar fuel tanks may result in frost or clear ice on the upper and/or lower surfaces of the wing spar-box or the spar-boxes of empennage surfaces if fuel is stored in the vertical or horizontal stabilizer. Typically this frost or clear ice will occur during descent and/or following landing with fuel that had been cold-soaked during cruise. Clear ice and frost resulting from cold-soaked fuel may occur even in warm, tropical ambient conditions, especially during periods of high humidity, and even rain, drizzle, or fog at ambient temperatures above freezing. Clear ice is difficult to detect prior to takeoff and may shed and be ingested into the engines for some aircraft designs or may cause structural damage. Engine ingestion of undetected clear ice and failure to remove frost from aircraft lifting surfaces have resulted in catastrophic accidents.

Failure to remove frost from the wing results in increased stall speeds and drag. Maximum lift may be reduced by 20 to 30 percent and stall speed margins at takeoff safety speeds may be significantly reduced. Increased drag from frost will reduce the rate-of-climb during takeoff, especially following an engine failure.

14 CFR §§ 91.527, 121.629, 125.221 and 135.227 state that no person may take off an aircraft when frost, ice, or snow is adhering to the wings, control surfaces, propellers, engine inlets, or other critical surface of the aircraft or when the takeoff would not be in compliance with other de/anti-icing and inspection requirements. 14 CFR § 121.629(b) states that takeoffs with frost under the wing in the area of the fuel tanks may be authorized by the Administrator. Under-wing frost typically results in increased drag and little or no adverse effects on stall speed. Fuselage frost to a thickness that does not obliterate painted markings may be acceptable. The applicant should substantiate that the effects of under-wing frost on airplane performance and handling qualities are not hazardous, and should define the degraded airplane flying qualities in the AFM. For some airplane designs frost may occur on the upper surface. 14 CFR §§ 91.527 and 135.227 allow takeoffs with frost on the wings or stabilizing or control surfaces if "that frost has been polished to make it smooth." Unless the applicant prohibits this procedure in the AFM Limitations section, the applicant should substantiate that the effects of "polished" frost on performance and flying qualities are not hazardous, and appropriate information should be added to the AFM.

The frost and clear ice must be removed from the upper surface and the surface should be protected from further development of frost by the application of anti-icing fluids. If ice or frost from a cold-soaked fuel condition could result in unsafe airplane operations, a "ground" ice detector(s) should be installed on the airplane upper surface on which frost or clear ice initially forms. Visual inspection aids, such as tufts and decals, are not acceptable since they do not provide an adequate means, or meet reliability requirements, for detection of ice on wing upper surfaces. A ground ice detection system does not relieve the operator from the requirement to show compliance with 14 CFR §§ 91.527, 121.629, 125.221 and 135.227, which require that the aircraft surfaces be free of frost, snow, and ice accumulation prior to takeoff.

The applicant should show that the ground ice detector system installed is of a kind and design appropriate for detecting cold-soaked fuel related wing ice and that it will ensure safe operation of the engines and airplane

components. The ground ice detector system must be labeled as to its function and/or limitations, and be installed according to limitations specified for the ice detector and related systems.

- The applicant should determine and reliably demonstrate the ice detector is installed in the wing area that will initially accumulate ice or frost due to cold-soaked wing fuel and the last place to melt this ice under any foreseeable operating conditions. The applicant should demonstrate that the ice detector is able to detect the formation of ice in that area reliably. Analysis, ground tests, laboratory tests, flight tests, or a combination of these may be used for these demonstrations.

- The applicant should show that the ice detector is in conformance with SAE AS5116.

- The ground ice detector should be installed such that it performs its intended function with considerations given to physical damage from foreign objects and damage during maintenance of the airplane.

- The ground ice detection system must detect ice caused by cold-soaked wing fuel in the following environmental conditions:

    - Outside air temperature from +20°C to -40°C.
    - Any atmospheric humidity
    - Frost
    - Snow (wet or dry)
    - Fog or freezing fog
    - Freezing drizzle
    - Light freezing rain
    - Rain

- The above detection capability in environmental conditions should be demonstrated:

    - With no anti-icing fluid
    - With each type of de/anti-icing fluid that will be approved for use on the airplane
    - With expected contaminants, such as engine fuel, lubricants, and hydraulic fluids.

- Proper function is defined as detection of clear ice with a thickness no greater than that that has been demonstrated not to pose a hazard to the airplane or engine operation.

- Flight test or vendor data may be used to demonstrate the detection capability in the defined environmental conditions.

- Nuisance alerts should be minimized and acceptable performance should be demonstrated during the flight test program.

- The effectiveness of the ice detector and its ability to perform its intended function reliably should be demonstrated by flight test under high humidity conditions with cold-soaked fuel:

- To verify the use of vendor data for the installed system and other information.
- To check the location of the ice detector.
- To demonstrate the effectiveness of the installed ice detector.
- To check for ice formation anomalies.

- AC 25.1309-1A and AC 23.1309-1C should be used for guidance on compliance with 14 CFR parts 23 and 25 § .1309,. The un-annunciated failure to detect ice due to cold soaked fuel on both wings is assumed to be a catastrophic failure condition, unless the characteristics of the airplane with clear ice on the upper wing surfaces are demonstrated to result in a less severe hazard category. The applicant should also evaluate the scenario where there is ice on only one wing and there is an annunciated failure to detect that ice. The annunciated failure of a ground ice detection system is considered to be minor and requires the operator to visually and physically check for upper wing ice.

- The amount of ice that develops on the wing upper surfaces prior to detection, caused by cold soaked fuel:
  - Should allow safe flight of the aircraft in accordance with 14 CFR part 33 § .77.
  - Should be accounted for in stall speeds and the associated operational speeds.
  - Should be shown not to degrade stall characteristics and stall warning below the standards established in 14 CFR parts 23 and 25 §§ .201, .203, and .207.

- The AFM should address:
  - Operational use of the ground ice detection system and limitations of the system.
  - Failure indications and associated crew procedures.

- The AFM should contain the following CAUTION:

  Ice shedding from the wing upper surface during takeoff can cause severe damage to one or both engines, leading to surge, vibration, or complete thrust loss. Ice can also degrade stall margins, stall characteristics, and airplane performance. The formation of ice can occur on wing surfaces during exposure of the airplane to normal icing conditions. Clear ice can also occur on the wing upper surfaces when the fuel in the wing fuel tanks is cold-soaked, and the airplane is exposed to conditions of high humidity, rain, drizzle, or fog at ambient temperatures well above freezing. Often, the ice accumulation is clear and difficult to detect visually. The ice forms most frequently on the top of the main wing tanks. The Ground Ice Detection System detects the formation of ice or frost only in this area. The Ground Ice Detection System does not detect ice, frost, or snow on other parts of the wing or airplane. The Ground Ice Detection System does not relieve the operator from the requirement to show compliance with 14 CFR §§ 91.527, 121.629, 125.221 and 135.227, which require that the aircraft surfaces be free of frost, snow, and ice accumulation prior to takeoff.